Scientia Iranica D (2019) 26(3), 1664–1689

Sharif University of Technology
Scientia Iranica
Transactions D: Computer Science & Engineering and Electrical Engineering
http://scientiairanica.sharif.edu

Quasi-reflection-based symbiotic organisms search algorithm for solving static optimal power flow problem

A. Saha*, A.K. Chakraborty, and P. Das

Department of Electrical Engineering, National Institute of Technology, Agartala, India.

Received 1 October 2016; received in revised form 20 February 2017; accepted 18 September 2017

KEYWORDS
OPF;
POZ;
Quadratic fuel cost function;
QRSOS;
SOS;
Valve-point loading.

Abstract. This paper offers a novel variant to the existing Symbiotic Organisms Search (SOS) algorithm to address the Optimal Power Flow (OPF) problems considering effects of valve-point loading (VE) and prohibited zones (POZ). Problem formulation includes minimization of cost, loss, Voltage Stability Index (VSI), Voltage Deviation (VD), and simultaneous minimization of their combinations. Quadratic cost function, effects of VE, and effects of both VE and POZ have been considered. OPF formulation considering effects of both VE and POZ is not yet available in the literature. Efficacy of SOS in resolving OPF is recognized in the literature. An opposition-based learning technique, named quasi-reflection, is merged into existing SOS to enhance its prospects of getting closer to superior quality solution. The proposed algorithm, named Quasi-Reflected Symbiotic Organisms Search (QRSOS), is assessed for IEEE 30 and IEEE 118 bus test systems. It shows promising results in reducing the objective function values of both systems by large margins (78.98% in case of VD when compared to SOS and NSGA-II and 46.06% in case of loss as compared to QOTLBO in IEEE 30 and IEEE 118 bus, respectively). QRSOS also outperformed its predecessors in terms of convergence speed and global search ability.

1. Introduction

Power systems are designed to deliver power to the loads in an efficient and economical manner. Due to the ever-increasing load demands, the ever-changing network parameters require existing systems to be more robust. OPF helps tune the existing network parameters in order to overcome various challenges faced by the system due to voltage instability, transmission capacity augmentation, transmission loss due to insufficient reactive power sources, etc. after satisfying diverse equality and inequality bounds. Equality bounds comprise power balance equations, whereas inequality bounds state the range of dependent and independent variables. The OPF is a non-linear and bounded optimization problem. A number of techniques for resolving the OPF problem are available in the literature. Techniques based on classical methods [1-8] include reduced gradient method, Newton-Raphson, Lagrangian relaxation, linear programming, and interior point method, to name a few. The main problem with classical optimization techniques is that they are too unable to achieve feasible solutions without making necessary approximations. However, approximations result in sub-optimal solutions. To overcome the limitations of classical methods, researchers have resorted to applying evolutionary algorithms for solving the OPF problem. The main advantage of evolutionary algorithms is that they are easy to formulate and are designed by studying the behavior of different organisms in nature. Moreover, they can adapt themselves to the problem by updating their population iteratively. Several heuristic algorithms have been

*. *Corresponding author.*
E-mail address: saha.anulekha@gmail.com (A. Saha)

doi: 10.24200/sci.2018.20179

projected for solving nonlinear OPF: Evolutionary Programming (EP) [9], Genetic Algorithm (GA) [10], Hybrid Evolutionary Programming (HEP) [11], Particle Swarm Optimization (PSO) [12], Differential Evolution algorithm (DE) [13], tabu search [14], Chaotic Ant Swarm Optimization Algorithm (CASOA) [15], Biogeography-Based Optimization (BBO) [16], Bacteria Foraging Optimization (BFO) [17], Harmony Search Algorithm (HSA) [18], Gravitational Search Algorithm (GSA) [19], teaching-learning-based algorithm (TLBO) [20], quasi-oppositional teaching-learning-based optimization (QOTLBO) [21], etc. Their efficacy has been proven.

For Multi-Objective Optimization (MOO), researchers have applied high-end soft-computing techniques with varying degrees of success. Abido [22] in 2011 used PSO to resolve the MOO. Pareto-based MOO techniques, such as TLBO and QOTLBO, were implemented to find the best conceding solution in [21]. In [23], a multi-objective genetic algorithm, based on NSGA-II, was applied to minimize voltage deviation, power loss, and the number of controls in a transmission network. In 2010, Roy et al. [24] implemented BBO algorithm for solving MOO OPF in 9, 26, and IEEE 118-bus systems [21]. In [25], Multi-Objective Harmony Search (MOHS) for the OPF problem was framed as a non-linear problem with constraints. Bhatacharya and Chattopadhyay [26] presented a Biogeography-Based Optimization (BBO) technique to solve OPF problems of a power system having generators with both non-convex and convex fuel cost characteristics. Cheng and Prayogo [27] proposed a new metaheuristic algorithm, named Symbiotic Organisms Search (SOS). In [28], Duman employed (SOS) to address OPF by considering VE and POZ. Opposition-based learning was first proposed by Tizhoosh [29] followed by the emergence of quasi-opposition-based learning by Rahnamayan et al. [30] which was found to give superior performance as compared to its predecessor. Ergezer et al. [31] proposed quasi-reflection-based learning that required the least computational work as compared to other opposition-based techniques. In [32] Zhang et al. proposed an enhanced version of the Opposition-Based PSO known as the Quasi-oppositional comprehensive learning PSO, which employed Opposition-Based Learning (OBL) for population initialization and selection. Instead of opposition numbers, the algorithm used quasi-opposite particles generated from the interval between the median and the opposite position of the particle. Applications of various evolutionary algorithms to OPF are demonstrated in [33-53], few of which also considered non-smooth cost functions. Wilcoxon [54] presented ranking methods for individual comparison. In [55,56] OPF considering POZs was solved. Abaci and Yamacli [57] used Differential Search Algorithm (DSA) for solving MOO-OPF problems. In [58] IEEE 118 bus data was presented. In [59-64] a solution to MOO-OPF using different evolutionary algorithms was presented. Ref. [65-70] dealt with solving OPF using incremental variables, glowworm swarm optimization, DE, and also with renewables including storage. In [71,72] reactive and economic power dispatch problems were solved using QOTLBO and BBO, respectively.

This paper presents a novel technique designated as quasi-reflected symbiotic organisms search (QRSOS) by applying opposition-based learning to the actual SOS [27] to address the OPF problem for different objectives. It is based on quasi-reflection, founded on opposite numbers theory and has already been proven mathematically of having the greatest possibility of an existing near-optimum solution when compared to all other opposition-based learning techniques [31]. To hasten the convergence of SOS, the present authors have incorporated the opposition-based learning scheme into the existing SOS.

The paper is divided into the following sections. Section 2 discusses formulation of OPF in detail. Section 3 presents a brief description of the existing SOS. Section 4 details a formulation of the proposed algorithm and its advantages over other meta-heuristic algorithms. Section 5 presents the simulation results and statistical analysis of the test results. Section 6 concludes the total work.

2. Construction of the OPF problem

The problem generally deals with defining the optimal parameter settings to minimize the total cost of fuel, subject to diverse equality as well as inequality constraints. The following equations may be used to express an OPF problem mathematically:

$$\min C(r, s), \tag{1}$$

$$\text{subject to } \; j(r, s) = 0, \tag{2}$$

$$\text{and } \; k(r, s) \leq 0, \tag{3}$$

where C is the objective for optimization, and s and r are vectors of independent and dependent variables, respectively.

Vector r involving slack bus power P_{G1}, load bus voltage V_{Li}, reactive power delivered by generator Q_{Gi}, and transmission line loading S_{Li} can be represented as follows:

$$r^T = \Big[P_{G1}, V_{L1}, ..., V_{LPQ}, Q_{G1}, ..., Q_{GPV}, S_{L1}, ..., S_{LTL}\Big]. \tag{4}$$

Vector of independent variables s involving generator

real power output, P_{Gi}, excluding the slack bus, generator bus voltage, V_{Gi}, shunt VAR compensator output, Q_{Ci}, transformer tap setting, T_{Ci}, can be represented as follows:

$$s^T = \Big[P_{G2},...,P_{GPV},V_{G1},...,V_{GPV},$$
$$Q_{C1},...,Q_{CNC},T_1,...,T_{NT}\Big], \quad (5)$$

where PQ, PV, NC, TL, and NT are the number of load buses, generator buses, compensators, transmission lines, and tap changing transformers, respectively.

Equality constraints set g, demonstrating load flow equations, may be stated as follows:

$$P_{Gi}-P_{Di}=V_i\sum_{k=1}^{NBUS}V_k\left(G_{ik}\cos\theta_{ik}+B_{ik}\cos\theta_{ik}\right), \quad (6)$$

where $i=1,2,3,...,NBUS$.

$$Q_{Gi}-Q_{Di}=V_i\sum_{k=1}^{NBUS}V_k\left(G_{ik}\sin\theta_{ik}+B_{ik}\cos\theta_{ik}\right), \quad (7)$$

where $i=1,2,3,...,NBUS$.

where P_{Gi} and Q_{Gi} are the real and reactive powers injected into the network, P_{Di} and Q_{Di} are the real and reactive power demands at the ith bus, G_{ik} and B_{ik} are conductance and susceptance, θ_{ik} is the difference between the phase angles of the voltages at the ith and kth buses, and NBUS is the overall number of buses comprising the system.

The following equations are representative of the set of inequality constraints h.

Generator limit constraints: The generator constraints are described below [21]:

$$V_{Gk}^{\min}\le V_{Gk}\le V_{Gk}^{\max}, \quad (8)$$

$$P_{Gk}^{\min}\le P_{Gk}\le P_{Gk}^{\max}, \qquad k=1,2,3,...,PV, \quad (9)$$

$$Q_{Gk}^{\min}\le Q_{Gk}\le Q_{Gk}^{\max}, \quad (10)$$

where PV is the total of generator buses counting the slack bus.

Transformer constraints: The transformer constraint is indicated as follows [21]:

$$T_k^{\min}\le T_k\le T_k^{\max}, \quad k=1,2,3,...,NT, \quad (11)$$

where NT represents the number of tap changing transformers.

Security constraints: These constraints involve lower and upper limits on the voltages of PQ buses as well as maximum line loadings and can be represented as follows [21]:

$$V_{Lk}^{\min}\le V_{Lk}\le V_{Lk}^{\max} \qquad k=1,2,3,...,PQ, \quad (12)$$

$$S_{Lk}\le S_{Lk}^{\max} \qquad k=1,2,3,...,TL, \quad (13)$$

where PQ and TL represent the total of load buses and transmission lines, respectively.

To keep the final output within operating bounds, the inequality constraints on the dependent variables are integrated within the objective function as quadratic penalty terms. To consider the security constraints, objective function (1) is modified as follows:

$$\begin{aligned}C_{\text{mod}} &= C+\lambda_P\left(P_{G1}-P_{G1}^{\text{bound}}\right)^2\\ &+\lambda_V\sum_{i=1}^{PQ}\left(V_{Li}-V_{Li}^{\text{bound}}\right)^2\\ &+\lambda_Q\sum_{i=1}^{PV}\left(Q_{Li}-Q_{Li}^{\text{bound}}\right)^2\\ &+\lambda_S\sum_{i=1}^{TL}\left(S_{Li}-S_{Li}^{\max}\right), \end{aligned} \quad (14)$$

where λ_P, λ_V, λ_Q, and λ_S are penalty factors, and x^{bound} is the limit value to which dependent variable x is set when limit violation occurs. It can be defined as follows:

$$\begin{cases}x^{\text{bound}}=x^{ub} & \text{when} \quad x>x^{ub}\\ x^{\text{bound}}=x^{lb} & \text{when} \quad x<x^{lb}\end{cases} \quad (15)$$

2.1. Objective functions

2.1.1. Single-objective functions

Generation cost minimization without VE and POZ

Generation cost represents the overall Fuel Cost (FC) expressed as a quadratic function of power [21,26]:

$$\begin{aligned}C_1=\min\left(F(P)\right)&=\left(\sum_{i=1}^{N_G}F_i\left(P_i\right)\right)\\ &=\left(\sum_{i=1}^{N_G}\left(a_i+b_iP_i+c_iP_i^2\right)\right),\end{aligned} \quad (16)$$

where P_i represents output power from generator i, and $F_i(P_i)$ denotes running cost of the ith generator; a_i, b_i, and c_i are the cost coefficients of the ith generating unit, and N_G is the number of generators committed. Eqs. (6) - (13) are the constraints on this objective.

FC minimization considering VE
This case is further divided into *Test case 2.1* and *Test case 2.2*. In both case studies, the following equation describes the VE [28]:

$$C_2 = \min\left(F(P)\right) = \left(\sum_{i=1}^{N_G} F_i\left(P_i\right)\right) = \left(\sum_{i=1}^{N_G}\left(a_i + b_i P_i + c_i P_i^2\right)\right) + \left|d_i \times \sin\left(e_i \times \left(P_{Gi}^{\min} - P_{Gi}\right)\right)\right|. \quad (17)$$

Cost minimization with POZ
POZs occur in thermal- or hydro-generating units due to confines of various power system components. Occurrence of POZ is mainly attributed to the shaft bearing vibration [35]. Frequency of vibration may equal the natural frequency causing resonance, thereby damaging the components. Generating units having POZ characterized by discontinuous input-output characteristics and operation in those areas are avoided for economic reasons. With reference to Figure 1, the POZs can be mathematically explained as follows:

$$P_{j,k}^{LB_k} \le P_j \le P_{j,k}^{UB_k}, \quad \forall j \in k = 1, 2, 3, ..., n, \quad (18)$$

where $P_{j,k}^{LB_k} = P_j^{\min}$, $P_{j,k}^{UB_k} = P_j^{\max}$, and n is the total POZ of each generating unit.

This case optimizes the Quadratic Fuel Cost (QFC) function in Eq. (16) considering POZs.

Cost minimization with VE and POZ
OPF problem is solved by considering effects of both VE and POZ for the cost function in Eq. (17).

Active power loss minimization
The objective of Real power Transmission Loss (RTL) is as follows [17]:

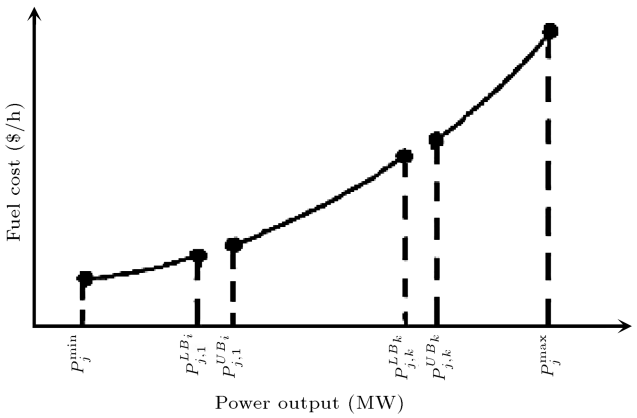

Figure 1. Representation of fuel cost with prohibited operating zones [56].

$$C_3 = \min(F(P_L)) = \sum_{m=1}^{N_L} G_m\left(V_j^2 + V_k^2 - 2V_j V_k \cos\theta_{jk}\right), \quad (19)$$

where G_m is conductance of line m connecting buses j and k; V_j and V_k represent, respectively, voltage magnitudes at buses j and k; N_L is the number of transmission lines; and θ_{jk} represents the angle difference between the two buses. Eqs. (6)-(13) are the constraints on this objective.

Voltage stability index (L-index) minimization
Mathematically, L-index of any node j can be expressed as follows [26,71]:

$$C_4 = \min(L_j)$$

$$L_j = \left|1 - \sum_{i=1}^{N_G} F_{ji}\frac{V_i}{V_j}\right|, \quad (20)$$

where $j = 1, 2, 3, ..., N_L$, and N_L is the number of load buses:

$$F_{ji} = -[Y_1]^{-1}[Y_2]^{-1},$$

where F_{ji} is the sub matrix attained after partially inverting $\mathrm{Y_{BUS}}$ matrix. Eqs. (6)-(13) represent constraints on this objective.

Voltage deviation minimization
Minimization of Voltage Deviation (VD) in all load buses from the reference voltage of 1 p.u. can be expressed as follows [26]:

$$C_5 = VD = \sum_{j=1}^{N_L}(V_j - V_j^{ref}), \quad (21)$$

where N_L denotes the total of load buses, V_j^{ref} is the stated reference value of voltage magnitude at the jth load bus and is commonly set to be 1.0 p.u. Eqs. (6)-(13) are the constraints.

Emission minimization
This objective considers minimizing the emission of all types of pollutants in the atmosphere. A linear model for emission minimization as provided in [21] has been considered for the sake of comparison. The constraints on this objective are (Eqs. (6)-(13)).

$$C_6 = \sum_{k=1}^{N_G}\delta_k P_k, \quad (22)$$

where δ_k represents emission coefficient relating to the kth generator.

2.1.2. Multi-objective functions (MOO)
Simultaneous minimization of QFC and RTL
This MOO is represented as follows:

$$C_{m1} = w_1 \times C_1 + (1 - w_1) \times C_3. \quad (23)$$

The objective function satisfies the constraints represented by Eqs. (6)-(13).

Minimization of FC along with RTL considering VE
This MOO function is represented by:

$$C_{m2} = w_1 \times C_2 + (1 - w_1) \times C_3. \quad (24)$$

Constraints of this case are presented in Eq. (6)-(13).

Minimizing FC along with RTL considering VE and POZ
The MOO function is denoted by Eq. (24). Constraints of this case are in Eqs. (6)-(13).

Minimizing FC along with VSI while neglecting the influence of VE and POZ
The MOO function in this case can be represented as follows:

$$C_{m3} = w_1 \times C_1 + (1 - w_1) \times C_4. \quad (25)$$

Eqs. (6)-(13) are the constraints on this objective.

Minimizing FC along with VSI considering VE.
The following equation represents the MOO function in this case:

$$C_{m4} = w_1 \times C_2 + (1 - w_1) \times C_4. \quad (26)$$

Eqs. (6)-(13) are the constraints of this objective.

Minimizing FC along with VSI considering VE and POZ
This MOO is described by Eq. (26). Eqs. (6)-(13) represent constraints on this objective function.

Minimizing FC along with VD while neglecting the effect of VE and POZ
This MOO function can be formulated as follows:

$$C_{m5} = w_1 \times C_1 + (1 - w_1) \times C_5, \quad (27)$$

where Eqs. (6)-(13) are the constraints.

Minimization of FC and VD considering the effect of VE
This multi-objective function is formulated as follows:

$$C_{m6} = w_1 \times C_2 + (1 - w_1) \times C_5, \quad (28)$$

where Eqs. (6)-(13) are the constraints to be satisfied.

Minimizing FC along with VD considering effects of VE as well as POZ
This multi-objective function is described using Eq. (28) and satisfies the constraints of Eqs. (6)-(13).

In the above multi-objective formulations, w_1 denotes weighting factor varying uniformly in the range (0,1). In this paper, the initial value of w_1 is set to 0 and, then, increases in steps of 0.1, i.e., the total range of (0,1) is divided into 10 intervals.

3. Symbiotic organisms search algorithm (SOS)

SOS described by Cheng and Prayogo [27] exploits the symbiotic relationship between organisms in nature. Three types of symbiosis exist in nature: mutualism, commensalism, and parasitism. The first relationship involves organisms that are mutually beneficial to each other; the second relationship involves organisms, in which one benefits and the other remains neutral of the association. In parasitism, one organism survives at the cost of the other.

3.1. Mutualism phase

Organism X_k matches the kth associate of the ecosystem. A new organism X_j is randomly chosen out of the ecosystem to interact with organism X_k. Both organisms get engaged in mutualism. New candidate solutions for the organisms after mutualism are calculated as follows [27]:

$$X_{knew} = X_k + (X_{best} - Mutual\_Vector * BF_1) * rand(0,1), \quad (29)$$

$$X_{jnew} = X_j + (X_{best} - Mutual\_Vector * BF_2) * rand(0,1), \quad (30)$$

$$Mutual\_Vector = \frac{X_k + X_j}{2}, \quad (31)$$

where $rand(0,1)$ represents a vector whose elements are random numbers. BF_1 and BF_2 denote the benefit factors that each organism has above the other. $Mutual\_Vector$ represents the mutualistic relationship.

Organisms involved in mutualism do not derive equal benefit from the association. One organism obtains greater benefits than the other. Benefit factors (BF_1 and BF_2) are chosen randomly as 1 or 2, denoting the degree of benefit to each organism, i.e., if an organism attains full or partial benefits due to this interaction.

3.2. Commensalism phase

Organism X_j is selected to interact with organism X_k acquired from the mutualism phase. In this phase, organism X_k tries to derive benefit from the interaction, while X_j remains neutral. X_k is updated only when its current fitness value is improved as compared to the previous fitness. Fitness of X_k is calculated as follows [27]:

$$X_{knew} = X_k + (X_{best} - X_j) * rand(-1,1). \quad (32)$$

3.3. Parasitism phase

Organism X_k creates a $Parasite\_Vector$ in the search

region. It is created by replicating and altering the dimensions of organism X_k with a random number. X_j acts as the host and is chosen randomly out of the ecosystem. Both $Parasite\_Vector$ and host X_j try to replace each other in the ecosystem; eventually, the one with a higher fitness value survives and replaces the other in the ecosystem.

4. Quasi-reflection-based learning

Quasi-reflection-based learning as proposed by Ergezer et al. [31] is briefly discussed below.

If x is any real number lying within the interval $[a, b]$ and $r = (a+b)/2$ denotes the center of the interval, then its quasi-reflected point x_{qref} can be expressed as follows [31]:

$$x_{qref} = rand(r, x), \tag{33}$$

where $rand(r, x)$ denotes a random number uniformly dispersed between r and x.

In an n-dimensional search space, the quasi-reflected point $QRP(x_1^{qr}, x_2^{qr}, x_3^{qr}, ..., x_k^{qr}, ..., x_n^{qr})$ of any point $P(x_1, x_2, x_3, ..., x_k, ..., x_n)$ may be defined as shown below:

$$x_k^{qr} = rand\left(\frac{a_k + b_k}{2}, x_k\right) \quad x_k \in [a, b]$$

$$k = 1, 2, 3, ..., n. \tag{34}$$

4.1. Quasi-reflected symbiotic organisms search algorithm (QRSOS)

QRSOS uses quasi-reflection-based learning for population initialization as well as generation jumping into SOS to accelerate the convergence rate. Jumping Rate (JR) is a control parameter set to jump or skip the creation of opposite population at certain generations, thereby saving computational time. Reflection Weight, RW, governs the amount of population reflection based on the solution fitness [72]. RW helps compare the weakest individuals with their extreme possible reflection, thereby reflecting the acceptable solutions to a nearby point. After generating the quasi-reflected population, the fitness function compares the present ecosystem with quasi-reflected ecosystem to select the fittest amongst them. The structure of the proposed QRSOS algorithm is described below:

Step 1: Create *ecosystem (E)* with a dimension, N_d, for specified ecosize and maximum function evaluation ($maxFE$) randomly within their operating limits based on Eqs. (8), (9), (11), and (12). *Ecosize* is determined by the number of generators, shunt compensators, and tap changing transformers. Elements of the ecosystem are identified as organisms, with each one being the representative of a contending solution to the problem. In addition, the ecosystem for pre-specified *ecosize* is initialized;

Step 2: Create a Quasi-Reflected Ecosystem (QRE) inside lower and upper bounds of control variables by employing Eq. (34);

Step 3: Assess fitness function for each organism set of the present ecosystem and the quasi-reflected ecosystem;

Step 4: Select N_E ($ecosize$) organisms from the present Ecosystem (E) as well as the quasi-reflected Ecosystem (QRE) based on their fitness;

Step 5: Update the ecosystem in each phase of SOS by Eqs. (29)-(32) using the concept of quasi-reflected opposition-based learning;

Step 6: By using Jumping Rate (JR), generate the quasi-reflected ecosystem for the ecosystem updated in Step 5 as described in Box I [72];

Step 7: Evaluate the fitness function of modified E and its QRE;

```
if rand < JR
  // Find the absolute of minimum, maximum, and median for the total ecosystem in the current generation.
  // Create reflection weight RW at the interval [0, 1], which determines the amount of reflection based on the
     fitness of an individual.
   for p = 1 : N_E
     for q = 1 : N_d
       if E_{p,q} < Median
         QRE_{p,q} = E_{p,q} + ((a_q + b_q)/2 − E_{p,q}) × RW
       else
         QRE_{p,q} = (a_q + b_q)/2 + (E_{p,q} − (a_q + b_q)/2) × RW
       end
     end
  end
end
```

Box I

Step 8: Select N_E number of the fittest organisms from E and QRE;

Step 9: Obtain *best fitness* and *best organism*. *Best fitness* denotes minimum of the fitness function assessed for each solution set, and *best organism* denotes the solution set for which *best fitness* is obtained;

Step 10: Go to Step 5 and repeat until *maxFE* is predefined. Store *best fitness* value in an array, identify the Pareto-optimal set, and store *best organism* in another array;

Step 11: For multi-objective formulations from Eqs. (23)-(28), change the value of weighting factor w_1 from 0 to 1 in steps of 0.1 and repeat Steps 1 to 10 till the value of w_1 reaches 1.

After altering the ecosystem in Steps 5 and 6, its feasibility should be tested, i.e., whether they satisfy the constraints given by Eqs. (8), (9), (11), and (12). If the organism set obtained is infeasible, they need to be mapped to a set of viable solutions in the following manner.

Let H_k be the kth control of OPF problem. If $H_k^{\max}$ and $H_k^{\min}$ denote respectively the upper and lower limits of the kth control variable. Then, the operating limit constraints are satisfied as mentioned below.

If output of the kth control variable $H_k > H_k^{\max}$,

$$\text{set} \quad H_k = H_k^{\max}.$$

If output of the kth control variable $H_k < H_k^{\min}$

$$\text{set} \quad H_k = H_k^{\min}.$$

After executing all three stages of QRSOS, if the dependent variables are found to violate their respective operational limits, then that organism set is discarded, and the three phases are reapplied to the old value till the operation limits and other constraints, if any, are satisfied.

For MOO functions, to attain the set for *best compromise* solution, fuzzy membership functions are analyzed to obtain the satisfactory non-dominated solution set. Membership function μ_{f_k} can be defined as follows [38]:

$$\begin{cases} \mu_{f_k} = 1 & f_k < f_k^{\min} \\ \frac{f_k^{\max} - f_k}{f_k^{\max} - f_k^{\min}} & f_k^{\min} < f_k < f_k^{\max} \\ 0 & f_k \geq f_k^{\max} \end{cases}$$

$$k = 1, 2, 3, ..., n, \tag{35}$$

where $f_k^{\min}$ and $f_k^{\max}$ denote respectively minimum and maximum objective function values. The effectiveness of each solution in satisfying the objectives is measured by calculating the total of the membership function values for all objectives. Normalization of membership functions is done in order to rate the efficacy of each non-dominated solution set with respect to all other non-dominated solution sets (m) and is calculated as follows:

$$\mu^j = \frac{\sum_{k=1}^{n} \mu_{f_k}^j}{\sum_{j=1}^{m} \sum_{k=1}^{n} \mu_{f_k}^j}. \tag{36}$$

The solution set with the maximum normalized membership μ^j value is considered as the *best non-dominated solution set.*

5. Results and discussion

The algorithm is coded using MATLAB R2014a and is executed with a PC equipped with Intel Core i7 processor clocked at 3.4 GHz and 2GB RAM. An *ecosize* of 30 is chosen to simulate the OPF program using QRSOS algorithm. Plots of fitness values of different objective functions are obtained over a span of 100 iterations in each case to analyze the convergence characteristics of QRSOS.

5.1. Description of the test system; IEEE 30 bus test system

Data and constraints of this system are obtained from [33-36]. Two sets of generator data and the corresponding prohibited zones (Tables 1 and 6 of Ref. [28]) have been used for analyzing the test cases.

5.2. Analysis of the results obtained using QRSOS

Results achieved using QRSOS are analyzed in detail in this sub-section. Bold fonts are used to represent the objective function values and the CPU time for computation.

5.2.1. Single-objective optimization for IEEE 30 bus test system

Test case 1: OPF problem neglecting effect of VE and POZ

Test case 1 considers the minimization of QFC described by (16) as its objective. Simulation results are demonstrated in Table 1. The optimized fuel cost using QRSOS is attained as 798.9299 $/hr. A comparative study of Test case 1 as shown in Table 2 reveals that QFC obtained using the proposed technique is lower than the best value of 801.5733 $/hr, as obtained using SOS [28]. In addition, the result obtained using the proposed algorithm is better than that obtained using other recently applied algorithms, such as Backtracking Search Algorithm (BSA), Artificial Bee Colony (ABC)

Table 1. Optimum control variable values for various test cases.

Control variables		Test case 1	Test case 2.1	Test case 2.2	Test case 3	Test case 4
Generator real power output (MW)	PG1	177	219.82	199.6	179.2	219.8
	PG2	48.664	27.851	20	45	27.96
	PG5	21.347	15.837	22.13	21.585	15.76
	PG8	21.062	10	27	22.889	10
	PG11	11.906	10	12.2	12.49	10
	PG13	12	12	12.36	11.533	12
Generator output voltage (p.u.)	VG1	1.1	1.0813	1.0778	1.0746	1.0811
	VG2	1.0881	1.05	1.05	1.05	1.05
	VG5	1.0628	1.0232	1.0247	1.0244	1.0237
	VG8	1.0694	1.0314	1.0366	1.0332	1.0316
	VG11	1.072	1.1	1.0995	1.1	1.0999
	VG13	1.1	1.05	1.0497	1.05	1.05
Transformer tap ratio	T6-9	0.98641	1.0998	1.0384	1.097	1.0997
	T6-10	1.0111	0.9191	0.9926	0.9063	0.9182
	T4-12	0.99402	0.9882	0.9949	0.9732	0.987
	T27-28	0.96114	0.9634	0.9694	0.9584	0.9634
Total fuel cost ($/hr)		**798.9299**	**825.2541**	**920.1125**	**801.7593**	**825.276**
Real power loss (MW)		8.5836	12.1087	9.8959	9.3009	12.1128
Voltage stability index (p.u.)		0.1062	0.1292	0.1298	0.1279	0.1291
Voltage deviation (p.u.)		2.0338	0.5703	0.5686	0.6818	0.5775
Simulation time (s)		**42.7342**	**87.5921**	**110.3562**	**120.4958**	**84.3752**

Table 2. Comparative study of Test case 1.

Technique	Fuel cost ($/hr)	Technique	Fuel cost ($/hr)
GA [41]	804.1000	HBMO [48]	802.2110
SA [41]	804.1000	EGA [38]	802.0600
GA-OPF[44]	803.9100	FGA [39]	802.0000
SGA [45]	803.6900	MHBMO [48]	801.9850
EP-OPF [44]	803.5700	SFLA [37]	801.9700
EP [46]	802.6200	PSO [36]	801.8900
ACO [47]	802.5700	Hybrid SFLA-SA [37]	801.7900
IEP [43]	802.4600	MPSO-SFLA [36]	801.7500
NLP [34]	802.4000	ABC [35]	801.7100
DE-OPF [42]	802.3900	BSA [35]	801.6300
MDE-OPF [42]	802.3700	SOS [28]	801.5730
TS [49]	802.2900	QRSOS	798.9152
MSFLA [40]	802.2870		

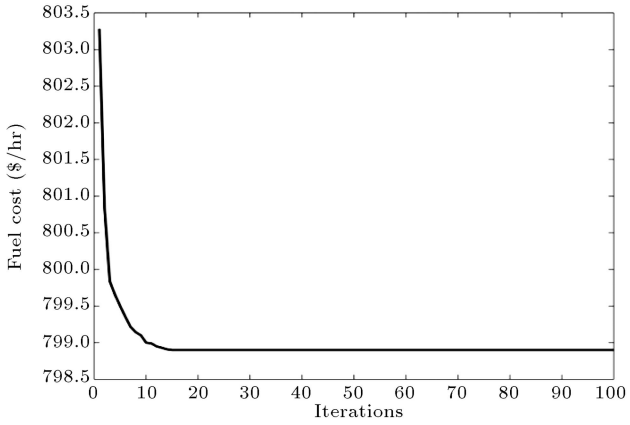

Figure 2. Convergence characteristic of Test case 1.

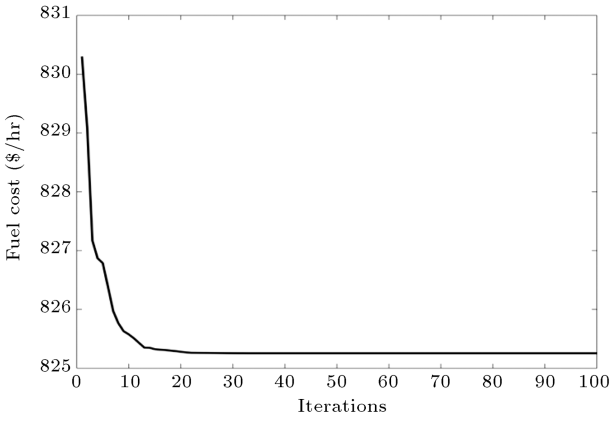

Figure 3. Convergence characteristic of Test case 2.1.

optimization, Modified Shuffle Frog Leaping Algorithm (MSFLA), etc., as available in the literature listed in Table 2. Figure 2 portrays the convergence characteristic of Test case 1. The algorithm converged in less than twenty iterations, showing faster convergence than its predecessor does.

Test case 2: OPF problem considering VE.

Test case 2.1

The result obtained for Test case 2.1 is provided in Table 1, which is derived by employing the generator cost coefficients as given in Table 1 of Ref. [28]. The cost function for this objective is formulated using Eq. (17). It is seen that the obtained FC considering VE and using QRSOS algorithm is 825.2541 $/hr. Comparative study of this test case has been done, as shown in Table 3. QRSOS provides better result than the previously obtained best value of 825.2985 $/hr, as achieved by SOS in [28]. Figure 3 depicts the convergence characteristics of this test case, and it is found to converge in less than thirty iterations.

Test case 2.2

Results of this test case are given in Table 1. The attained FC is 920.1125 $/hr considering valve effect, using QRSOS algorithm, and generator cost coefficients as provided in Table 6 of Ref. [28]. The cost function is described by Eq. (17). Comparative study is provided in Table 4, which substantiates that the proposed algorithm achieves better result than others to which it is compared. Figure 4 depicts the convergence characteristics of this case, and it is found to converge

Table 3. Comparative study of Test case 2.1.

Technique	Fuel cost ($/hr)	Technique	Fuel cost ($/hr)
RCGA [50]	831.0400	Hybrid SFLA-SA [37]	825.6921
GA [50]	829.4493	ABC [35]	825.6000
SA [37]	827.8262	BSA [35]	825.2300
PSO [37]	826.5897	SOS [28]	825.2985
DE [37]	826.5400	QRSOS	825.2541
SFLA [37]	825.9906		

Table 4. Comparative study of Test case 2.2.

Technique	Fuel cost ($/hr)	Technique	Fuel cost ($/hr)
GA [51]	996.0369	ABC [53]	928.4370
GA-APO [51]	996.0369	PSO [54]	925.7581
NSOA [51]	984.9365	MSG-HS [54]	925.6410
ITS [43]	969.1090	IABC [55]	921.8265
TS-SA [43]	959.5630	IABC-LS [55]	921.8235
EP [43]	955.5080	BSA [35]	921.3570
IEP [43]	953.5730	SOS [28]	921.3288
SADE-ALM [52]	944.0310	QRSOS	920.1125

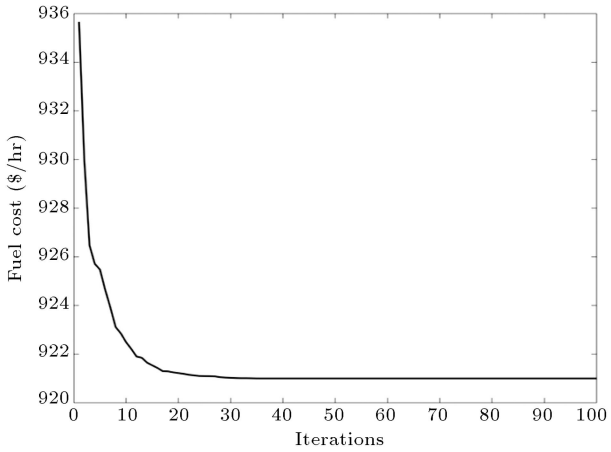

Figure 4. Convergence characteristic of Test case 2.2.

in about thirty iterations, which is less than one-sixth of that required by SOS [28].

Test case 3: OPF considering POZ

Generator cost coefficients as provided in Table 1 of Ref. [28] and QFC of Eq. (16) are considered. Obtained results of this test case are provided in Table 4. Table 5 provides a comparative study of this test case. QRSOS reduces objective function value to 801.7593 $/hr from the previously obtained best value of 801.8398 $/hr in [28]. Figure 5 depicts the convergence characteristics of this method that shows faster convergence in less than 45 iterations, which is nearly 36.36% of that required by SOS in [28].

Test case 4: OPF problem considering both VE and POZ

Generator cost coefficients provided in Table 1 of [28] and cost function as described by Eq. (17) are considered. The result of this case is tabulated in Table 1.

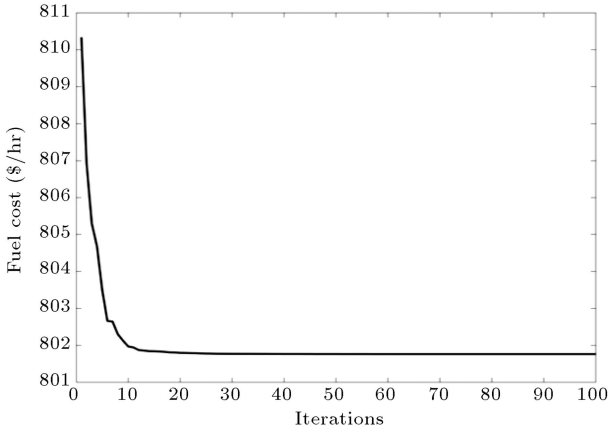

Figure 5. Convergence characteristic of Test case 3.

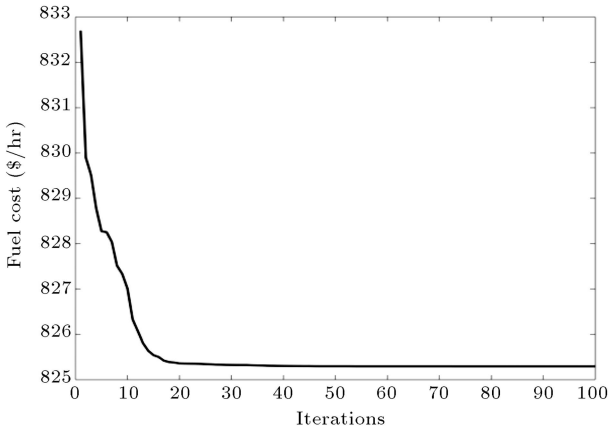

Figure 6. Convergence characteristic of Test case 4.

Comparative study of this objective is presented in Table 6, demonstrating competitiveness of the proposed algorithm to achieve lower cost. Figure 6 shows a faster convergence curve of this test case when compared to SOS [28].

Table 5. Comparative study of Test case 3.

Technique	Fuel cost ($/hr)	Technique	Fuel cost ($/hr)
GA [37]	809.2314	ABC [35]	804.3800
SA [37]	808.7174	BSA [35]	801.8500
PSO [37]	806.4331	SOS [28]	801.8398
SFLA [37]	806.2155	QRSOS	801.7593
Hybrid SFLA-SA [37]	805.8152		

Table 6. Comparative study of Test case 4.

Technique	Fuel cost ($/hr)	Technique	Fuel cost ($/hr)
GA [37]	838.1727	ABC [35]	831.6500
SA [37]	836.5364	BSA [35]	826.3700
PSO [37]	835.4785	SOS [28]	825.3705
SFLA [37]	834.8165	QRSOS	825.2760
Hybrid SFLA-SA [37]	834.6339		

Table 7. Comparative study of Test case 5.

	Control variables	QRSOS	QOTLBO [21]	TLBO [21]	MOHS [25]	DSA [57]
Generator real power output (MW)	PG1	51.244	51.3093	52.1027	52.5327	51.0945
	PG2	79.999	80	79.9387	79.5432	80
	PG5	50	49.9794	49.9617	49.8152	50
	PG8	35	34.9959	34.5287	34.7403	35
	PG11	30	29.9988	29.9721	29.7884	30
	PG13	40	40	39.8304	39.948	40
Generator output voltage (p.u.)	VG1	1.1	1.087	1.0798	1.0754	1.0605
	VG2	1.0981	1.0825	1.0742	1.0728	1.0566
	VG5	1.0803	1.0632	1.0557	1.054	1.0378
	VG8	1.0872	1.0707	1.0641	1.0637	1.0453
	VG11	1.0712	1.0998	1.0976	1.0991	1.1
	VG13	1.1	1.0989	1.0989	1.0967	1.0474
Shunt compensator injection (p.u.)	QC10	2.81E-05	0.0495	0.0498	0.0499	0.05
	QC12	0.0499	0.0499	0.0498	0.0486	0.05
	QC15	0.0498	0.0297	0.0497	0.0493	0.05
	QC17	0.0498	0.0499	0.0498	0.0488	0.05
	QC20	0.0421	0.0387	0.0403	0.0442	0.05
	QC21	0.0499	0.05	0.0496	0.0499	0.05
	QC23	0.0213	0.0273	0.0267	0.0411	0.0422
	QC24	0.0312	0.05	0.0497	0.0499	0.05
	QC29	0.0235	0.0207	0.0212	0.0317	0.0303
Transformer tap ratio	T6-9	1.0199	1.0309	1.0171	1.0022	1.0329
	T6-10	0.9773	0.9024	0.9	0.9078	0.9993
	T4-12	0.9864	0.9689	0.9681	0.9593	0.9913
	T28-27	0.9741	0.9584	0.9527	0.9533	0.9786
Cost($/h)		967.0473	967.0371	965.7677	964.5121	967.6493
Transmission loss (MW)		**2.8436**	2.8834	2.9343	2.9678	3.0945
Voltage stability index (p.u.)		0.1074	0.1262	0.1264	0.1154	0.12604

Test case 5: OPF problem with the objective of RTL minimization

Objective of this test case is formulated using Eq. (19). Table 7 lists the optimal control variables of this objective.

The suggested algorithm is capable of bringing down loss to 2.8423 MW, which is lower than that obtained using QOTLBO, TLBO, MOHS, and DSA in the literature. In addition, the result obtained using QRSOS is 1.42% lower than the previous best result of 2.8834 MW [21]. For this case, QRSOS took less than 35 iterations to converge, which is lower than that observed in [21] as depicted in Figure 7.

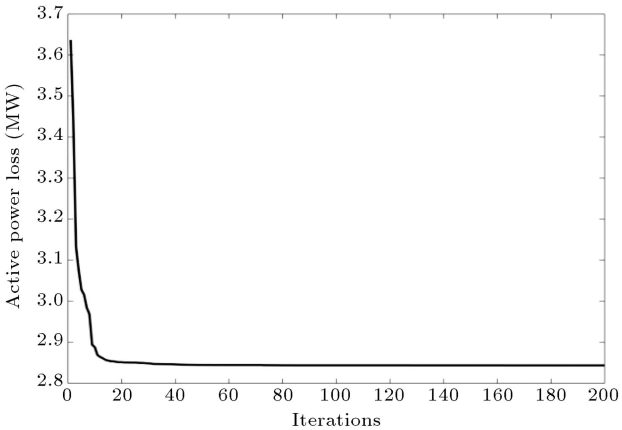

Figure 7. Convergence characteristic of Test case 5.

Table 8. Comparative study of Test case 6.

	Control variables	QRSOS	QOTLBO [21]	TLBO [21]	MOHS [25]	DSA [57]
Generator real power output (MW)	PG1	157.54	134.2408	76.788	92.6114	64.0725
	PG2	40.938	61.8427	63.3618	67.5094	67.5711
	PG5	15	15	45.7092	48.8891	50
	PG8	10	10	33.8121	34.8663	35
	PG11	29.994	29.9687	29.9842	29.7139	30
	PG13	39.965	39.6304	37.4921	14.134	40
Generator output voltage (p.u.)	VG1	1.0705	1.0832	1.0601	1.0993	1.06
	VG2	1.0444	1.0666	1.0463	1.0986	1.0549
	VG5	0.9894	1.0426	1.043	1.0973	1.0316
	VG8	1.0603	1.0389	1.0443	1.0998	1.0399
	VG11	1.1	1.0938	1.0986	1.0984	1.0778
	VG13	0.9695	1.0976	1.0926	1.0996	1.0709
Shunt compensator injection (p.u.)	QC10	0.0499	0.0492	0.0463	0.0499	0.0393
	QC12	0.0499	0.0499	0.0487	0.0492	0.05
	QC15	0.0498	0.0369	0.0497	0.0496	0.05
	QC17	0.05	0.05	0.0426	0.0499	0.05
	QC20	0.0499	0.0187	0.0437	0.05	0.05
	QC21	0.05	0.0042	0.0434	0.0497	0.05
	QC23	0.0485	0.0009	0.0193	0.0494	0.0406
	QC24	0.0499	0.0005	0.0051	0.0494	0.05
	QC29	0.0178	0.0011	0.0406	0.0496	0.0286
Transformer tap ratio	T6-9	1.0999	0.9288	0.9646	0.9027	0.9989
	T6-10	1.0985	0.9	0.9602	0.9001	1.0046
	T4-12	1.1	0.9442	0.92	0.9036	1.0368
	T28-27	0.9002	0.9082	0.9256	0.9011	0.9792
Cost ($/h)		843.8153	844.1237	912.5914	895.6223	944.4086
Transmission Loss (MW)		10.0412	7.2826	3.7474	4.3244	3.24373
L-index (p.u.)		**0.092613**	0.0994	0.1003	0.1006	0.12734

Test case 6: OPF for L-index minimization
This case considers lowering L-index value to improve voltage stability of the system using Eq. (20). Control parameters of this case are listed in Table 8.

It can be observed that the proposed methodology lowers the value of this objective function to 0.092613 p.u., which is the lowest of those obtained using QOTLBO, TLBO, MOHS, and DSA. In addition, it lowered the L-index value by 6.82% from the previous best-reported value of 0.0994 p.u. [21]. Figure 8 shows a quicker rate of convergence for this case, too.

Test case 7: Voltage Deviation (VD) minimization
This test case considers improving the load voltage profile of the system using Eq. (21). Optimal control parameters attained for this case are listed in Table 9.

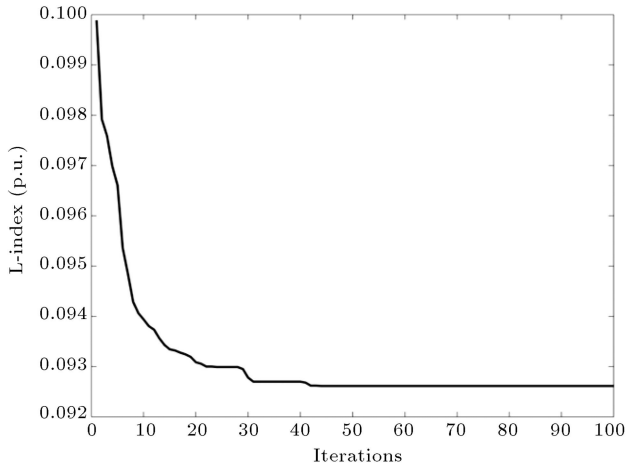

Figure 8. Convergence characteristic of Test case 6.

Table 9. Comparative study of Test case 5.

	Control variables	QRSOS	NSGA-II [23]
Generator real power output (MW)	PG1	0.5247	×
	PG2	0.8	×
	PG5	0.5	×
	PG8	0.35	×
	PG11	0.2978	×
	PG13	0.4	×
Generator output voltage (p.u.)	VG1	1.0009	1.03
	VG2	1.0016	1.03
	VG5	1.0179	1
	VG8	1.0084	1
	VG11	0.9767	1.02
	VG13	1.0059	1.04
Shunt compensator injection (p.u.)	QC10	0.9897	×
	QC12	0.9697	×
	QC15	0.9855	×
	QC17	0.9758	×
	QC20	0.0021	×
	QC21	0.027	×
	QC23	0.0499	×
	QC24	0	×
	QC29	0.05	×
Transformer tap ratio	T6-9	0.0448	1
	T6-10	0.049	1.01
	T4-12	0.0499	1
	T28-27	0.0341	1.04
Voltage deviation (p.u.)		**0.0798**	0.38
Transmission loss (MW)		3.8676	5.3513

QRSOS lowered the VD value to 0.079866 p.u. by a high margin of 78.98% as compared to NSGA-II in [23]. The transmission loss is also reduced to a great extent. The algorithm converged within 25 iterations for this test case as observed in Figure 9.

5.2.2. Single-objective optimization for IEEE 118 bus test system

To check the competence of the offered algorithm in a large system, IEEE 118 bus test system is taken into consideration for studying different test cases. Data of the system are obtained from [58]. Penalty factors have been assigned to the objectives as per Eq. (14) to handle the possible constraint violations of this large system. The penalty factors are considered in the range

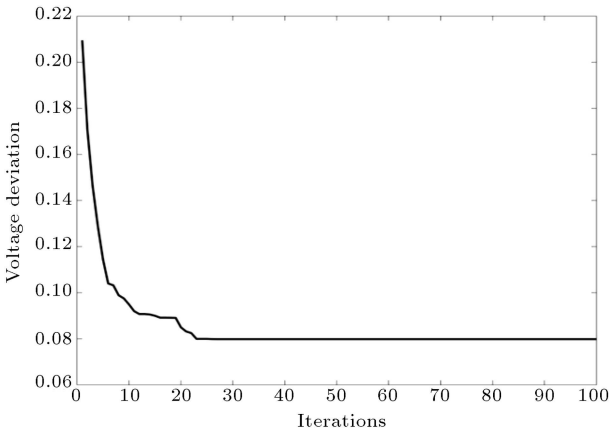

Figure 9. Convergence characteristic of Test case 7.

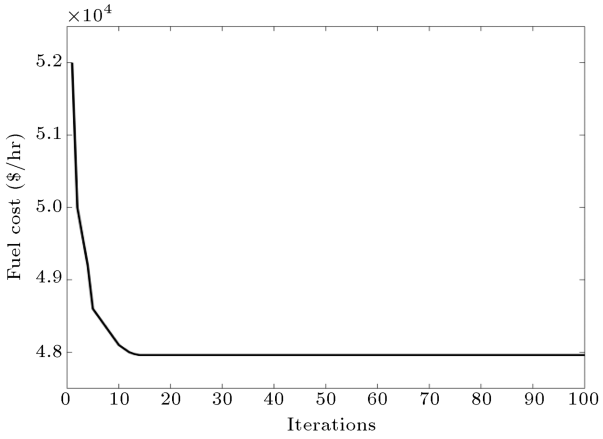

Figure 10. Convergence characteristic of Test case 8 obtained using QRSOS.

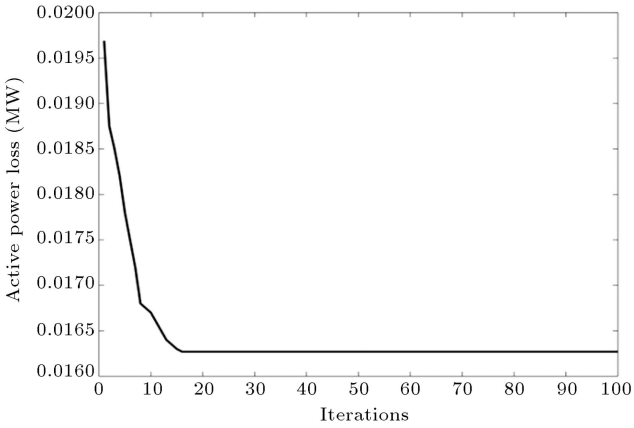

Figure 11. Convergence characteristic of Test case 9.

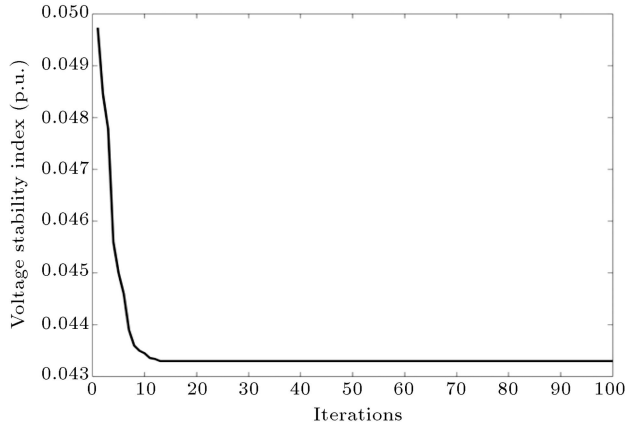

Figure 12. Convergence characteristic of Test case 10.

of [10000 100000], and tuning has been done in steps of 10000. Results of all penalty factors are not shown here for page limitations. Optimum results have been obtained for a penalty factor of 30000 assigned to the objectives, which are tabulated in the subsequent test cases:

Test case 8: OPF problem for QFC minimization
Optimal results are obtained for a penalty factor of 30000 assigned to the objective. The results and their comparisons are provided in Table 10.

As can be observed from Table 10, QRSOS effectively reduced the fuel cost by a large margin of 14.30% from 55,968.14 $/hr [21] to 47,960 $/hr. In addition, it effectively reduced the emission from 410.9816 lb/hr [21] to a much lower value of 342.635 lb/hr in the case of single-objective optimization itself. It achieved better results than those of QOTLBO and TLBO in [21]. The proposed algorithm showed rapid convergence in less than 20 iterations, as seen in Figure 10.

Test case 9: OPF problem for real power transmission loss minimization
This test case minimized the real power loss occurring during transmission using Eq. (18). A penalty factor of 30000 assigned to the loss minimization objective gave optimum results, which are listed in Table 11.

QRSOS is proficient in reducing the transmission loss to 16.27 MW, nearly half of that of 35.3191 MW and 36.8482 MW obtained respectively by QOTLBO and TLBO, as reported in [21]. Simultaneously, it is also able to reduce the emission by 6.5127 lb/hr compared to that obtained by QOTLBO. Figure 11 shows rapid convergence in less than 20 iterations.

Test case 10: OPF problem for minimizing L-index
L-index of large IEEE 118 bus has been considered to improve voltage profile using Eq. (19). Since it is very difficult to maintain the voltage stability in case of a large system, a penalty factor of 30000 has been assigned to the objective to handle inequality constraints. Optimum control parameters obtained for this test case are listed in Table 12.

Optimal value of VSI is obtained as 0.0433 p.u., which denotes a stable system. Figure 12 shows the convergence characteristic of Test case 10. Convergence is achieved in less than 15 iterations.

Test case 11: OPF problem for emission minimization objective
This test case considers minimizing emission of pollutants to the atmosphere. The objective is formulated using Eq. (21). A penalty factor of 30000 assigned to the objective provided optimal results while effectively handling the constraints. Optimal parameters of this test case are listed in Table 13.

QRSOS provided the lowest emission value when compared to those obtained using QOTLBO and TLBO. It effectively reduced the emission from 176.1666 lb/hr in [21] to 164.5 lb/hr, i.e., by a margin of 6.62%. In addition, it reduced the fuel cost by 3.29% from 65,601.64 $/hr [21] and transmission loss by 7.58% from the previously reported best value of

Table 10. Comparative study of Test case 8.

	Control variables	QRSOS	QOTLBO [21]	TLBO [21]		Control variables	QRSOS	QOTLBO [21]	TLBO [21]
Generator real power output (MW)	PG1	29	5.0513	5.0374	Generator output voltage (p.u.)	VG26	1.0278	1.0596	1.0518
	PG4	5	5.0223	5.0318		VG27	1.0825	1.0512	1.0406
	PG6	5.0254	5.0187	5.1436		VG31	1.0494	1.0575	1.049
	PG8	150.01	150.3032	150.7002		VG32	1.0588	1.0394	1.0329
	PG10	100.06	169.3889	171.3829		VG34	0.9608	1.0389	1.03
	PG12	10.001	10.0213	10.0116		VG36	0.9537	1.0323	1.0271
	PG15	25.055	25.2916	25.1637		VG40	0.9163	1.0366	1.0374
	PG18	5.0034	5.0674.0	5		VG42	0.937	1.0291	1.0417
	PG19	5.0016	5	5.0182		VG46	1.0096	1.0412	1.0551
	PG24	100.01	120.1963	120.4126		VG49	0.9627	1.0237	1.0453
	PG25	349.91	349.5982	349.7829		VG54	0.9388	1.0197	1.0424
	PG26	8.0025	8.0623	8.0728		VG55	0.9347	1.0206	1.0431
	PG27	9.6979	8.0846	8.1045		VG56	0.9368	1.0241	1.046
	PG31	25.003	25.0722	25.1863		VG59	0.9439	1.0309	1.0533
	PG32	8.0045	8.0192	8.1232		VG61	1.01	1.0288	1.0513
	PG34	99.985	25.1262	25.1527		VG62	0.999	1.0699	1.0696
	PG36	8.0117	8.0206	8.0528		VG65	1.0506	1.0431	1.061
	PG40	8.0038	8.0448	8.2236		VG66	0.9829	1.038	1.0362
	PG42	25.325	25.0537	25.3548		VG69	0.9426	1.053	1.0525
	PG46	50.015	249.6018	249.0325		VG70	0.9884	1.0572	1.0542
	PG49	50.514	249.9137	248.1637		VG72	1.0406	1.042	1.0399
	PG54	25	25.2048	25.1607		VG73	1.0245	1.0243	1.0217
	PG55	25	25.0768	25.4524		VG74	0.9591	1.0194	1.0163
	PG56	50.004	199.9312	198.7935		VG76	0.9568	1.0327	1.0271
	PG59	50	199.7859	199.8001		VG77	1.009	1.0423	1.0343
	PG61	25.002	25.042	25.5916		VG80	1.0496	1.0886	1.0892
	PG62	100.01	327.0837	326.3556		VG85	1.0316	1.0199	1.02
	PG65	420	319.6931	314.8521		VG87	1.0619	1.0897	1.0898
	PG66	30.043	30.1746	30.2394		VG89	1.0423	1.0366	1.0266
	PG69	29	110.9331	115.4795		VG90	1.0231	1.0305	1.0185
	PG70	10.003	10.0207	10.2128		VG91	1.0311	1.0363	1.0256
	PG72	5.0124	5.0423	5.1262		VG92	1.0348	1.0386	1.0286
	PG73	5	5.0288	5.0132		VG99	0.9697	1.0545	1.0456
	PG74	25.003	25.3524	25.1628		VG100	0.9993	1.0402	1.0296
	PG76	25.125	25.0485	25.1246		VG103	0.9971	1.0346	1.023
	PG77	299.95	150.3722	150.6738		VG104	1.0084	1.0297	1.019
	PG80	25.054	25.0812	25.0102		VG105	1.0113	1.0278	1.0161
	PG85	10.002	10.0242	10.1632		VG107	1.0315	1.0215	1.0087
	PG87	100.04	183.8538	183.7419		VG110	0.97	1.0346	1.0243
	PG89	50.084	97.2006	95.8227		VG111	0.981	1.0411	1.0298
	PG90	8.0001	8	8.0211		VG112	0.9261	1.0345	1.0256
	PG91	47.302	20.0123	20.1013		VG113	0.9519	1.0615	1.0501
	PG92	214.8	103.6475	104.3625		VG116	1.1	1.0679	1.0677
	PG99	100	100.0325	100.1091	Shunt compensator injection (p.u.)	QC34	0.0901	0.0663	0.2668
	PG100	100.05	114.7707	113.6624		QC44	0.2995	0.0516	0.0507
	PG103	8.0138	8.0188	8.0586		QC45	0.1203	0.2169	0.2236
	PG104	25.084	25.0423	25.3061		QC46	0.2285	0.0086	0.2494
	PG105	25.001	25.2536	25.1527		QC48	0.2964	0.0846	0.081
	PG107	8.0026	8.0091	8.0143		QC74	0.2678	0.1156	0.1583
	PG110	25	25.0222	25.2862		QC79	3.13E-06	0.2996	0.298
	PG111	25.123	25.0547	25.0384		QC82	0.2927	0.2997	0.2998
	PG112	25.368	25.0117	25.2232		QC83	0.0176	0.0979	0.1099
	PG113	25.003	25.1642	25.2035		QC105	0.2996	0.0989	0.1729
	PG116	25.001	25.0107	25.0643		QC107	0.1983	0.1616	0.0879
Generator output voltage (p.u.)	VG1	1.083	1.0607	1.0496		QC110	0.1892	0.1008	0.1388
	VG4	0.9625	1.0546	1.0413	Transformer tap ratio	T8-5	0.9369	1.0042	1.0121
	VG6	0.9661	1.0857	1.0841		T26-25	1.0599	1.0999	1.0998
	VG8	0.9945	1.0895	1.09		T30-17	1.0922	1.0182	1.0275
	VG10	1.1	1.0524	1.0419		T38-37	1.0731	1.0265	1.0315
	VG12	0.9735	1.0467	1.0352		T63-59	1.0534	1.0378	1.0159
	VG15	0.9531	1.0505	1.0385		T64-61	0.9342	1.0311	1.0086
	VG18	0.9384	1.0452	1.0343		T65-66	1.0379	0.9002	0.9
	VG19	0.9459	1.0712	1.0658		T68-69	0.9	0.9961	0.9945
	VG24	1.0839	1.09	1.0897		T81-80	0.9	1.0042	1.0113
	VG25	1.0419	1.09	1.0896		**Fuel cost ($/hr)**	**47,960**	55,968.14	55,989.87
						Emission (lb/hr)	342.635	410.9816	410.5538

Table 11. Comparative study of Test case 9.

	Control variables	QRSOS	QOTLBO [21]	TLBO [21]		Control variables	QRSOS	QOTLBO [21]	TLBO [21]
Generator real power output (MW)	PG1	29.728	29.8931	14.1548	Generator output voltage (p.u.)	VG27	0.9477	1.0344	0.9982
	PG4	17.57	20.7667	23.0473		VG31	0.9472	1.0399	0.9874
	PG6	5.0015	23.5384	25.2495		VG32	0.9476	1.0247	1.0123
	PG8	150	160.8306	161.4631		VG34	0.9713	1.025	1.0166
	PG10	298.92	105.1021	202.4847		VG36	0.9653	1.0138	1.0136
	PG12	10.387	29.1323	29.1093		VG40	0.9586	1.0387	1.0146
	PG15	41.455	87.5141	94.3115		VG42	0.9713	1.0371	1.0554
	PG18	5.8168	8.1933	23.9002		VG46	0.99	1.0337	1.0439
	PG19	5	23.0788	15.1346		VG49	0.9874	1.039	1.0544
	PG24	100.01	147.7714	113.9182		VG54	0.9954	1.0454	1.0525
	PG25	100.09	126.8438	100.3799		VG55	0.9932	1.0399	1.0529
	PG26	8.0177	22.9912	22.1332		VG56	0.9933	1.0382	1.0199
	PG27	8.0197	28.5314	27.1458		VG59	0.9635	1.0544	1.0123
	PG31	54.483	78.2105	87.9738		VG61	1.0046	1.0527	1.008
	PG32	18.793	20.1445	29.6566		VG62	0.9987	1.0538	1.0512
	PG34	43.155	83.2007	78.1281		VG65	1.0354	1.0462	1.027
	PG36	29.929	24.6842	28.9505		VG66	0.9854	1.0162	1.0134
	PG40	29.853	20.4124	29.0852		VG69	1.0152	1.0277	1.0175
	PG42	99.967	94.9384	87.2005		VG70	1.0413	1.0367	1.0061
	PG46	75.876	58.6024	127.8746		VG72	1.0281	1.0244	1.0065
	PG49	173.17	236.2374	93.3376		VG73	1.0693	1.0039	1.0032
	PG54	99.992	80.436	59.2742		VG74	1.0232	1.0077	1.0056
	PG55	68.862	97.7809	71.2112		VG76	1.0049	1.0107	0.989
	PG56	168.52	77.1155	136.8644		VG77	1.0061	1.0191	1.0036
	PG59	199.99	179.9903	97.9237		VG80	0.9958	1.0069	0.9844
	PG61	25.004	76.5748	58.1055		VG85	1.0382	1.0126	1.0103
	PG62	100	185.5016	336.6485		VG87	1.0998	1.0818	1.0797
	PG65	419.48	192.6547	142.6236		VG89	1.0539	1.0387	1.0511
	PG66	30.345	78.8729	79.8481		VG90	1.0393	1.0382	1.0438
	PG69	29.728	80.0818	95.1218		VG91	1.038	1.0407	1.0497
	PG70	29.898	10.9715	10.1947		VG92	1.0418	1.0357	1.0369
	PG72	5.001	20.1172	19.8263		VG99	0.9898	1.0393	1.051
	PG73	18.818	19.9734	10.6108		VG100	0.9915	1.0273	1.043
	PG74	99.348	89.9006	97.7145		VG103	0.9894	1.0193	1.0661
	PG76	99.571	88.5942	31.0182		VG104	0.9818	1.0113	1.0361
	PG77	274.26	227.4576	185.5746		VG105	0.9876	1.0094	1.0323
	PG80	100	30.4116	44.2247		VG107	0.968	1.0078	1.0318
	PG85	26.926	14.0215	11.3845		VG110	1.0205	1.0155	1.0311
	PG87	100.32	100.1543	107.1638		VG111	1.0208	1.0198	1.0368
	PG89	50.911	57.9964	61.6745		VG112	1.0421	1.0219	1.0349
	PG90	19.989	12.4839	10.6637		VG113	0.9515	1.0347	1.0207
	PG91	44.355	24.0536	23.5206		VG116	1.0138	1.0505	1.072
	PG92	273.51	100.3382	115.7448	Shunt compensator injection (p.u.)	QC34	0.2718	0.117	0.105
	PG99	100.04	105.0007	119.2147		QC44	0.0036	0.0404	0.0019
	PG100	100.07	107.3321	105.7234		QC45	0.2997	0.2089	0.2249
	PG103	12.4	11.9027	8.1071		QC46	0.2272	0.274	0.1187
	PG104	25	27.5847	40.6412		QC48	0.0053	0.0744	0.0558
	PG105	99.627	28.8382	45.4382		QC74	0.1768	0.0844	0.1757
	PG107	11.383	13.3147	18.1017		QC79	0.231	0.2919	0.2922
	PG110	50	31.3725	29.1604		QC82	0.0235	0.2949	0.245
	PG111	25	25.2184	25.2835		QC83	0.1119	0.0931	0.1293
	PG112	74.902	35.8435	31.7249		QC105	0.0027	0.155	0.1657
	PG113	59.328	56.6809	80.6904		QC107	0.298	0.1093	0.0988
	PG116	49.523	49.2005	44.257		QC110	0.0087	0.0965	0.0926
Generator output voltage (p.u.)	VG1	0.9809	1.051	1.0202	Transformer tap ratio	T8-5	0.9484	0.9941	1.0113
	VG4	1.005	1.0434	1.0214		T26-25	1.0418	0.9026	1.0515
	VG6	0.9951	1.0701	1.0499		T30-17	0.9649	1.0364	1.0292
	VG8	0.9735	1.0755	1.0557		T38-37	1.0303	1.0087	1.0112
	VG10	1.0416	1.0367	1.0148		T63-59	1.0664	1.0081	1.0128
	VG12	0.9824	1.0221	1.0188		T64-61	0.9674	0.9929	1.0674
	VG15	0.955	1.0265	1.0159		T65-66	1.0576	0.9045	1.0588
	VG18	0.9431	1.0181	1.0133		T68-69	0.9682	0.9881	1.033
	VG19	0.9461	1.0468	1.0063		T81-80	0.9884	1.0138	1.0538
	VG24	1.0096	1.0541	1.0088		Fuel cost ($/hr)	70,963	63,693.91	63,515.12
	VG25	0.9889	1.0897	1.0756		Emission (lb/hr)	373.2768	379.7895	318.0176
	VG26	0.9686	1.0413	0.994		**Transmission loss (MW)**	**16.27**	35.3191*	36.8482

*The unit of the result obtained using QOTLBO for loss minimization in [21] is given as kW, whereas the real value comes as 35.3191 MW after calculation using the parameters provided by the authors.

Table 12. Optimal parameter settings for Test case 10.

	Control variables	QRSOS		Control variables	QRSOS		Control variables	QRSOS
Generator real power output (MW)	PG1	29.977	Generator real power output (MW)	PG100	133.29	Generator output voltage (p.u.)	VG76	0.985
	PG4	24.303		PG103	19.349		VG77	1.0591
	PG6	13.342		PG104	87.283		VG80	1.083
	PG8	227.14		PG105	82.227		VG85	0.989
	PG10	169.09		PG107	11.192		VG87	0.9
	PG12	24.426		PG110	50		VG89	1.0385
	PG15	69.884		PG111	99.971		VG90	1.0265
	PG18	17.269		PG112	99.699		VG91	1.0421
	PG19	22.526		PG113	25.099		VG92	1.0391
	PG24	100.01		PG116	37.44		VG99	0.9857
	PG25	100.03	Generator output voltage (p.u.)	VG1	0.9859		VG100	1.0148
	PG26	17.521		VG4	1.0128		VG103	1.0162
	PG27	8		VG6	1.0283		VG104	1.0262
	PG31	83.334		VG8	1.005		VG105	1.0343
	PG32	11.171		VG10	1.1		VG107	1.088
	PG34	25		VG12	1.0256		VG110	1.0014
	PG36	8.3366		VG15	1.0251		VG111	0.983
	PG40	29.907		VG18	1.0362		VG112	1.0011
	PG42	95.503		VG19	1.0185		VG113	1.0364
	PG46	146.37		VG24	0.9331		VG116	1.0147
	PG49	249.95		VG25	1.0085	Shunt compensator injection (p.u.)	QC34	0.1929
	PG54	97.799		VG26	1.0144		QC44	0.3
	PG55	72.019		VG27	0.9639		QC45	0.3
	PG56	199.95		VG31	0.9814		QC46	0.2573
	PG59	75.556		VG32	0.9754		QC48	0.0075
	PG61	35.641		VG34	0.9809		QC74	0.1588
	PG62	177		VG36	0.9769		QC79	0.2771
	PG65	412.18		VG40	0.9		QC82	0.2923
	PG66	139.44		VG42	1.0999		QC83	0.0084
	PG69	29.977		VG46	1.1		QC105	0.2824
	PG70	16.165		VG49	1.0782		QC107	0.0997
	PG72	12.618		VG54	0.9683		QC110	0.1069
	PG73	12.863		VG55	0.978	Transformer tap ratio	T8-5	0.9364
	PG74	42.698		VG56	0.9785		T26-25	1.0443
	PG76	26.457		VG59	1.0104		T30-17	0.9246
	PG77	210.27		VG61	0.9983		T38-37	1.1
	PG80	28.485		VG62	1.0093		T63-59	0.9553
	PG85	25.111		VG65	1.0592		T64-61	1.0221
	PG87	178.32		VG66	1.025		T65-66	1.0498
	PG89	83.092		VG69	1.0341		T68-69	0.9643
	PG90	19.851		VG70	0.9909		T81-80	0.9555
	PG91	49.548		VG72	0.9385		Fuel cost ($/hr)	72,309
	PG92	204.51		VG73	0.9767		Transmission loss (MW)	103.81
	PG99	108.94		VG74	0.9908		**L-index (p.u.)**	**0.0433**

150.9366 MW [21], simultaneously. Figure 13 shows the convergence for this case.

5.2.3. Bi-objective results for IEEE 30 bus test system
Nine different case studies have been carried out on the IEEE 30 bus test system for diverse MOO functions, and their pareto-fronts have been studied.

A Pareto optimal solution is defined as the finest solution set selected from numerous solution sets in which all objectives are equally compromised with respect to one another. Each solution set is defined as a non-dominated solution set. There can be an infinite number of Pareto solution sets for a multi-objective optimization problem.

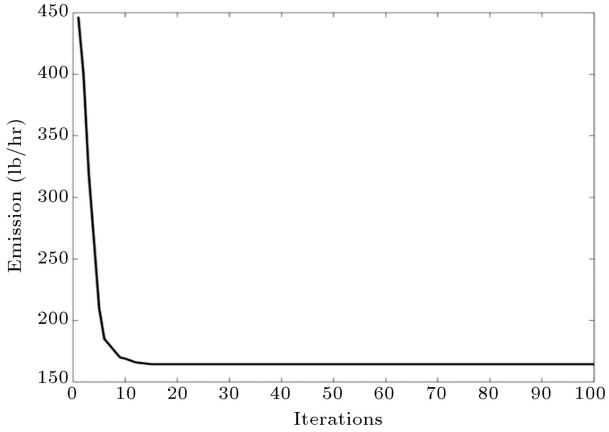

Figure 13. Convergence characteristic of Test case 11.

Table 13. Comparative study of Test case 11 for QRSOS.

	Control variables	QRSOS	QOTLBO[21]	TLBO[21]		Control variables	QRSOS	QOTLBO[21]	TLBO[21]
Generator real power output (MW)	PG1	29	30	13.1937	Generator output voltage (p.u.)	VG27	1.0882	1.0272	1.0426
	PG4	11.361	29.9302	28.7162		VG31	1.0442	1.0338	1.0469
	PG6	29.983	29.8782	18.4882		VG32	1.0657	1.0395	1.0453
	PG8	150	299.8738	270.3844		VG34	0.9849	1.0375	1.0397
	PG10	100.64	142.7617	264.8307		VG36	0.978	1.0249	1.0496
	PG12	29.714	22.0728	29.1476		VG40	0.9348	1.0278	1.0571
	PG15	91.021	44.0345	35.9218		VG42	0.9203	1.037	1.0694
	PG18	5	5	5		VG46	0.9708	1.0373	1.0714
	PG19	5	5.0111	5		VG49	0.9947	0.9948	1.0702
	PG24	100	100.4435	100.4172		VG54	0.9451	1.049	1.0877
	PG25	100	100.4082	100		VG55	0.9471	1.0261	1.0736
	PG26	8.1201	26.9576	29.3547		VG56	0.9471	1.0526	1.0845
	PG27	8.7412	12.112	28.2438		VG59	0.9598	1.0403	1.0883
	PG31	67.54	97.9324	83.8513		VG61	1.012	1.031	1.0674
	PG32	8	8.0141	8.0142		VG62	1.0163	1.0648	1.0663
	PG34	25	25.0213	25.0202		VG65	1.0287	1.0456	1.0851
	PG36	8	8	8.0134		VG66	0.9994	1.0304	1.0203
	PG40	8	8	8.0283		VG69	0.9454	1.039	1.0349
	PG42	32.46	99.6537	26.8744		VG70	0.9681	1.0406	1.042
	PG46	249.95	179.4485	126.7132		VG72	1.053	1.0333	1.0233
	PG49	50	50.0503	50.0483		VG73	1.0027	1.0143	1.0106
	PG54	25	25.0728	25.1737		VG74	0.9424	1.0193	1.0072
	PG55	25	25.0137	25.4218		VG76	0.951	1.0386	1.0291
	PG56	50	50.0234	50.3506		VG77	1.0113	1.0629	1.0351
	PG59	199.99	123.5961	132.1043		VG80	1.0464	1.0899	1.0842
	PG61	38.07	84.2513	33.5485		VG85	1.0087	1.0146	1.0199
	PG62	420	173.6788	254.15		VG87	1.063	1.0898	1.0871
	PG65	80	80	80		VG89	1.0419	1.0428	1.0291
	PG66	30	30.331	32.3293		VG90	1.0971	1.0415	1.0244
	PG69	29	80.0753	107.9949		VG91	1.0322	1.0524	1.0381
	PG70	10	10.2342	10.1963		VG92	1.0337	1.0537	1.0424
	PG72	5	5.4008	10.5836		VG99	0.9764	1.0281	1.0883
	PG73	5	5.6437	5.3809		VG100	1.0075	1.0706	1.0706
	PG74	25	27.8556	25.5065		VG103	1.0086	1.0791	1.0743
	PG76	25	27.6722	30.1247		VG104	1.0215	1.0631	1.043
	PG77	240.34	272.0213	237.3293		VG105	1.0206	1.062	1.0447
	PG80	84.397	70.0576	63.4527		VG107	1.0566	1.0513	1.0255
	PG85	13.542	28.1374	19.2557		VG110	0.9757	1.0824	1.0256
	PG87	179.01	181.63	299.4339		VG111	1.0213	1.0798	1.0492
	PG89	113.86	144.6645	155.9003		VG112	0.9107	1.0865	1.0417
	PG90	15.976	16.9528	19.6379		VG113	0.9662	1.0522	1.053
	PG91	45.96	44.9324	41.5361		VG116	1.0521	1.0805	1.0739
	PG92	196.58	147.4587	114.5003	Shunt compensator injection (p.u.)	QC34	0.2999	0.1784	0.29
	PG99	265.61	172	131.9728		QC44	0.1811	0.0462	0.0421
	PG100	246.91	213.1142	175.3218		QC45	0.1032	0.2032	0.1844
	PG103	11.754	19.4834	15.8526		QC46	0.0029	0.057	0.0233
	PG104	74.106	80.2192	95.8003		QC48	0.0438	0.0766	0.0679
	PG105	67.72	73.9628	83.2438		QC74	0.1116	0.1794	0.2857
	PG107	14.257	19.7113	18.4581		QC79	0.0336	0.2993	0.297
	PG110	48.915	48.6485	46.4433		QC82	0.3	0.2925	0.0962
	PG111	31.689	85.3081	99.9002		QC83	1.57E-06	0.2999	0.287
	PG112	83.836	83.2133	90.2355		QC105	0.0627	0.0487	0.197
	PG113	33.722	67.1145	95.4081		QC107	0.1428	0.2225	0.2103
	PG116	34.93	41.9238	29.7641		QC110	0.0007	0.0043	0.1421
Generator output voltage (p.u.)	VG1	1.0597	1.0327	1.0191	Transformer tap ratio	T8-5	0.987	1.0119	1.017
	VG4	0.9347	1.0254	1.0222		T26-25	0.9243	1.0989	1.0992
	VG6	0.9593	1.072	1.0606		T30-17	1.0706	1.0134	1.0133
	VG8	1.0014	1.0788	1.0775		T38-37	1.0145	1.0021	0.989
	VG10	1.0859	1.0208	1.0258		T63-59	0.961	0.9761	1.0046
	VG12	0.9831	1.0373	1.0333		T64-61	0.9181	1.0315	0.9929
	VG15	0.9674	1.0342	1.0374		T65-66	1.0442	0.9612	0.9003
	VG18	0.9569	1.0319	1.036		T68-69	0.9417	1.0321	1.0927
	VG19	0.962	1.0449	1.0446		T81-80	0.9003	1.0116	1.0368
	VG24	1.0996	1.0529	1.0583		Fuel cost ($/hr)	**63,441**	65,601.64	65,037.34
	VG25	1.1	1.0766	1.078		**Emission (lb/hr)**	**164.5**	176.1666	182.9609
	VG26	1.0156	1.0319	1.0311		Transmission loss (MW)	**139.49**	150.9366	188.5034

Test case 12: OPF problem for simultaneously minimizing QFC and RTL

This objective function is described using Eq. (23), and results are presented in Table 14. The comparative study, as depicted in Table 15, showed that the algorithm achieved better result than those obtained using MO-DEA, QOTLBO, TLBO, MOHS, and NSGA-II in the literature. Compared to MO-DEA, QRSOS lowered the transmission loss from 5.5949 MW [64] by 1.69% to 5.5002 MW. However, at the same time, the total FC increased by a small margin of 0.071%. It was observed that VSI value improved simultaneously,

Table 14. Optimum control variable settings for different test cases for bi-objective functions.

	Control variables	Case12	Case13	Case14	Case15	Case16	Case17	Case18	Case19	Case20
Generator real power output (MW)	PG1	1.2849	1.9356	2.1982	1.7688	1.9456	2.1981	1.7658	1.9249	2.1903
	PG2	0.517	0.4513	0.2756	0.4873	0.4899	0.2842	0.4895	0.4677	0.2861
	PG5	0.2967	0.2067	0.1609	0.2138	0.1862	0.1557	0.2154	0.1986	0.1688
	PG8	0.35	0.1183	0.1	0.2114	0.1	0.1	0.2218	0.1425	0.1
	PG11	0.2448	0.1	0.1	0.1186	0.1	0.0974	0.1191	0.1	0.1246
	PG13	0.1958	0.12	0.1202	0.12	0.12	0.12	0.12	0.12	0.098
Generator output voltage (p.u.)	VG1	1.1	1.1	1.081	1.1	1.1	1.0813	1.0485	1.0186	1.029
	VG2	1.0904	1.0824	1.05	1.0873	1.0791	1.05	1.0289	1.0047	1.0282
	VG5	1.0673	1.0566	1.0233	1.0615	1.0632	1.0234	1.0062	1.0181	1.0191
	VG8	1.0773	1.064	1.0316	1.069	1.0562	1.0316	1.0049	1.0093	0.9959
	VG11	1.0813	1.0926	1.0985	1.0768	1.1	1.1	0.9857	1.0001	1.0593
	VG13	1.1	1.1	1.05	1.1	1.0582	1.05	0.9859	0.9976	1.0219
Shunt compensator injection (p.u.)	QC10	0.0125	0.0125	—	0.05	0.05	—	0.05	0.0023	—
	QC12	0.0498	0.05	—	0.05	0.0427	—	0	0.0346	—
	QC15	0.05	0.0499	—	0.05	0.0446	—	0.05	0.05	—
	QC17	0.05	0.05	—	0.05	0.0367	—	0	0	—
	QC20	0.0429	0.0442	—	0.05	0.0066	—	0.05	0.05	—
	QC21	0.05	0.0499	—	0.0499	0.0447	—	0.0294	0.0434	—
	QC23	0.0183	0.022	—	0.0223	0.0233	—	0.045	0.0469	—
	QC24	0.0383	0.0402	—	0.0427	0.0144	—	0.05	0.05	—
	QC29	0.0234	0.0243	—	0.0201	0	—	0.02	0.0345	—
Transformer tap ratio	T6-9	1.0102	1.0772	1.0997	1.0429	1.0368	1.1	1.002	1.0145	1.086
	T6-10	0.9812	0.9032	0.9168	0.9493	1.0976	0.9127	0.9889	0.9712	0.9
	T4-12	0.9756	0.9677	0.987	0.9712	1.0997	0.9832	0.9439	0.9652	0.9586
	T27-28	0.9645	0.9579	0.9625	0.9574	0.9038	0.9572	0.968	0.9804	0.9419
Fuel cost ($/hr)		**821.4655**	**833.3756**	**825.2938**	**799.0175**	**835.2983**	**825.4182**	**803.3138**	**842.5288**	**832.7439**
Real power loss (MW)		**5.5002**	**9.7887**	**12.0904**	8.7768	10.7703	12.1405	10.0139	11.97 4	13.3898
Voltage stability index (p.u.)		0.1185	0.1081	0.129	**0.1067**	**0.1072**	**0.1277**	0.1446	11.974	0.135
Voltage deviation (p.u.)		1.6125	1.9877	0.5796	1.5026	0.9079	0.6268	**0.0991**	**0.0832**	**0.1461**
Simulation time (s)		59.6103	62.566	72.4231	52.352	68.203	76.5432	59.246	63.2024	61.0255

Table 15. Comparative study of Test case 12.

Technique	Fuel cost ($/hr)	Real power loss (MW)	Voltage stability index (p.u.)
MOHS [25]	832.6709	5.3143	NA
NSGA-II [23]	823.8875	5.7699	NA
TLBO [21]	828.5300	5.2883	0.1259
QOTLBO [21]	826.4954	5.2727	0.1255
MO-DEA [64]	820.8802	5.5949	NA
QRSOS	**821.4655**	**5.5002**	0.1185

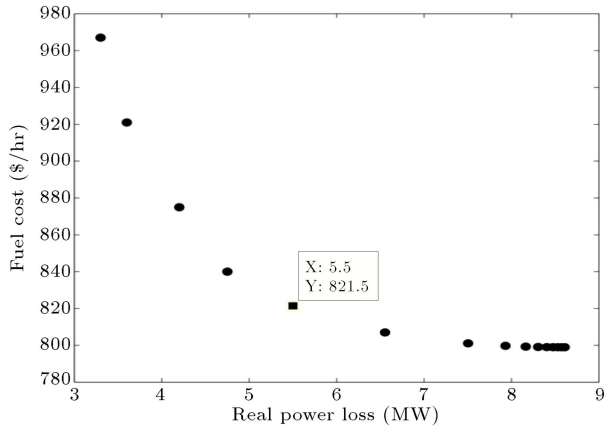

Figure 14. Pareto front for Test case 12.

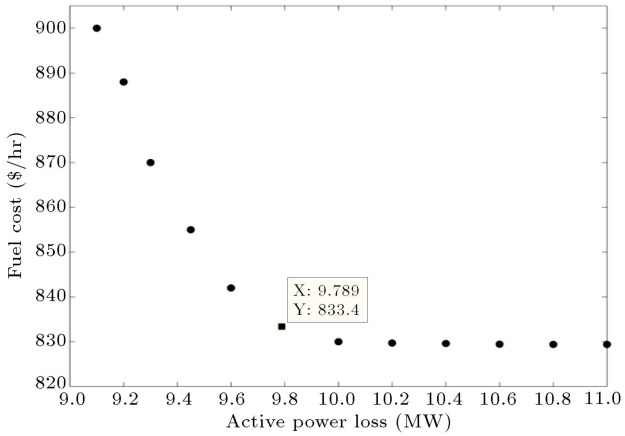

Figure 15. Pareto front for Test case 13.

thereby increasing the voltage stability margin. Figure 14 depicts the Pareto-front obtained for the above objective.

Test case 13: OPF for simultaneously minimizing FC and RTL considering VE

Generator cost coefficients provided in Table 1 of [28] are used for this objective described using Eq. (24). Results are presented in Table 14. The total FC attained using QRSOS is 833.3756 $/hr, which is 0.98% higher than that of Case 2.1, and the RTL is 9.7887 MW, which is 19.16% lower than that of Case 2.1. Figure 15 represents the Pareto front obtained for Test case 13. No existing results are available in the literature for doing comparative study.

Test case 14: OPF for minimizing FC along with RTL considering both VE and POZ

Generator cost coefficients and the POZs, as provided in Table 1 of Ref. [28], are used in Eq. (24). Based on Table 14, it can be witnessed that total FC is 825.2938 $/hr and the RTL is 12.0904 MW. The total FC increased with a slight margin of 0.002% and RTL reduced by 0.18% when compared to single-objective minimization of Test case 4. Figure 16 represents the Pareto-front for this test case. No existing results are available in the literature for doing comparative study.

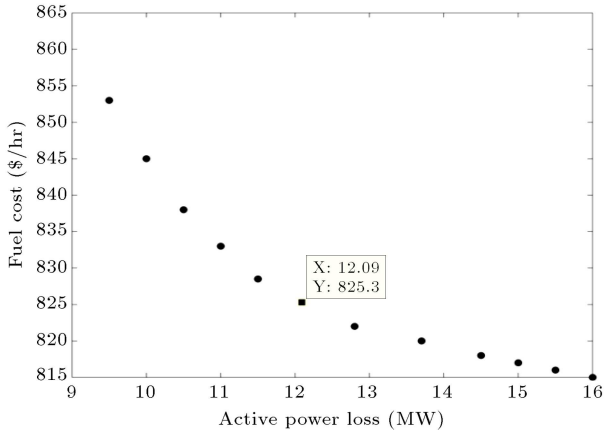

Figure 16. Pareto front for Test case 14.

Test case 15: OPF for simultaneously minimizing QFC and L-index neglecting VE and POZ

This objective function is described using Eq. (25). Table 14 demonstrates results obtained for this bi-objective function. According to Table 16, QRSOS reduced the total QFC to 799.0175 $/hr, which is lower than those obtained using QOTLBO, TLBO, NSGA-II, and MOHS, and recently applied BSA and MO-DEA in the literature. Based on the comparison of the result with those of the latest algorithms such as BSA [63] and MO-DEA [64], it is observed that QRSOS

Table 16. Comparative study of Test case 15.

Technique	Fuel cost ($/hr)	Real power loss (p.u.)	Voltage stability index (p.u.)	Voltage deviation (p.u.)
MOHS [25]	799.9401	NA	0.1075	NA
NSGA-II [23]	800.3170	NA	0.1083	NA
TLBO [21]	799.8564	8.8592	0.1270	NA
QOTLBO [21]	799.3415	8.7050	0.1256	NA
BSA [63]	800.3340	8.4904	0.1259	1.9855
MO-DEA [64]	799.6912	8.602	0.1249	2.0498
QRSOS	799.0175	8.7768	0.1067	1.5026

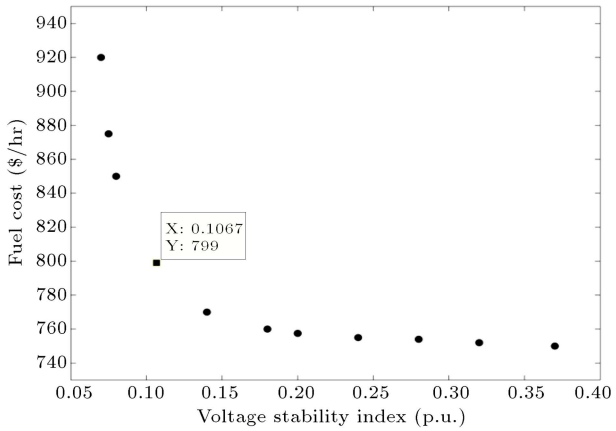

Figure 17. Pareto front for Test case 15.

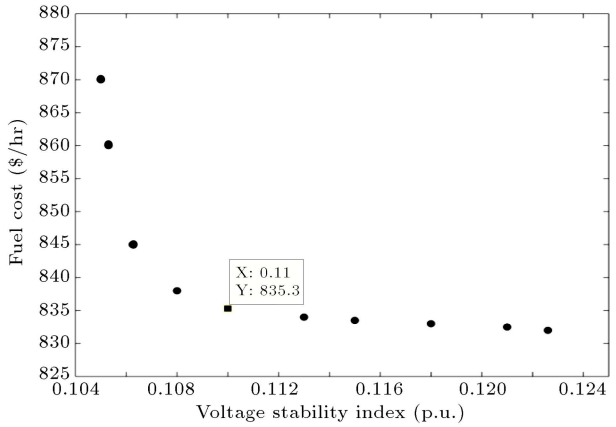

Figure 18. Pareto front for Test case 16.

lowers the QFC value by 0.0803%. Simultaneously, it can lower the VSI value to 0.1067 p.u. by 15.25% from the latest MO-DEA [64], thereby ensuring a stable system. Figure 17 represents the Pareto front for this bi-objective function.

Test case 16: OPF for simultaneously minimizing FC and VSI considering VE

Generator cost coefficients as provided in Table 1 of [28] are used for this case described by Eq. (26). Results attained for this test case are tabulated in Table 14. Figure 18 shows the Pareto-front for this objective function. Overall, the FC for this bi-objective function came out to be 835.2938 $/hr and the VSI as 0.1072 p.u. The FC increased by a negligible margin of 1.21% and the VSI reduced by 17.70% when compared to single-objective minimization of Test case 2.1. No existing results are available in the literature for comparison.

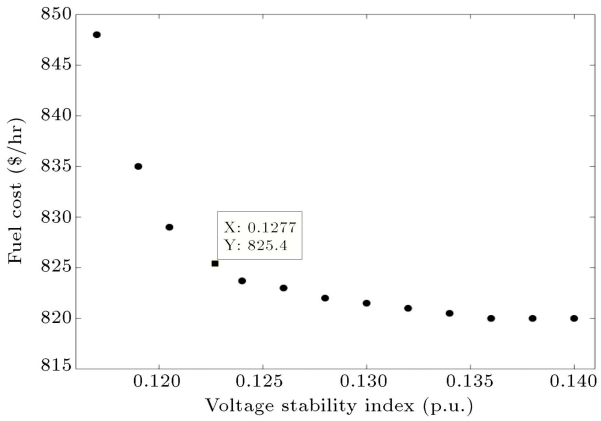

Figure 19. Pareto front for Test case 17 obtained using QRSOS.

Test case 17: OPF for simultaneously minimizing FC and VSI considering VE and POZ

Generator cost coefficients and POZs as provided in Table 1 of [28] are used for test case described by Eq. (26). Results obtained for this test case are demonstrated in Table 14. QRSOS achieved FC of 825.4182 $/hr and VSI of 0.1277 p.u. The total FC increased by a negligible margin of 0.017%, whereas the VSI improved by a margin of 1.08% when compared to single-objective minimization of Test case 4. Figure 19 represents the Pareto-front for this case. No existing results are available in the literature for comparison.

Test case 18: OPF for minimizing QFC along with VD

This objective function is defined using Eq. (27). Results obtained for this test case are demonstrated in Table 14. VD obtained using QRSOS is 0.0991 p.u. which is 94.09% lower, and the total FC is 803.3138 $/hr which is 0.55% higher when compared to single-objective minimization of Test case 1. In addition, when compared to the recently applied techniques, such as BSA [63] and MO-DEA [64], it is observed from Table 17 that QRSOS lowers the FC as well as VD by 0.074% and 14.42%, respectively. Figure 20 depicts the Pareto front for this test case.

Test case 19: OPF to minimize FC along with VD considering VE

Generator cost coefficients from Table 1 of [28] are

Table 17. Comparative study of Test case 18.

Technique	Fuel cost ($/hr)	Voltage deviation (p.u.)
BSA [63]	803.4294	0.1147
MO-DEA [64]	803.9116	0.1158
QRSOS	**803.3138**	**0.0991**

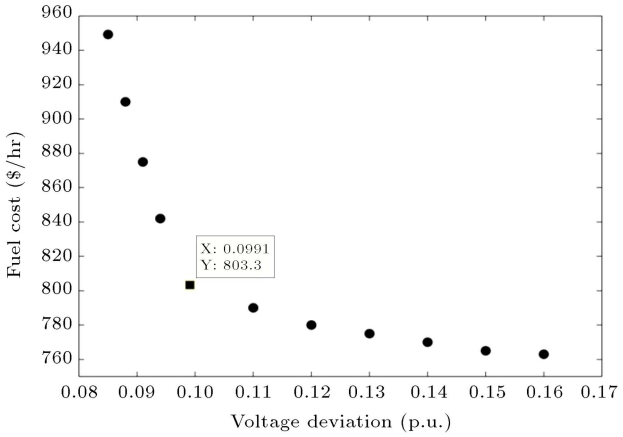

Figure 20. Pareto front for Test case 18.

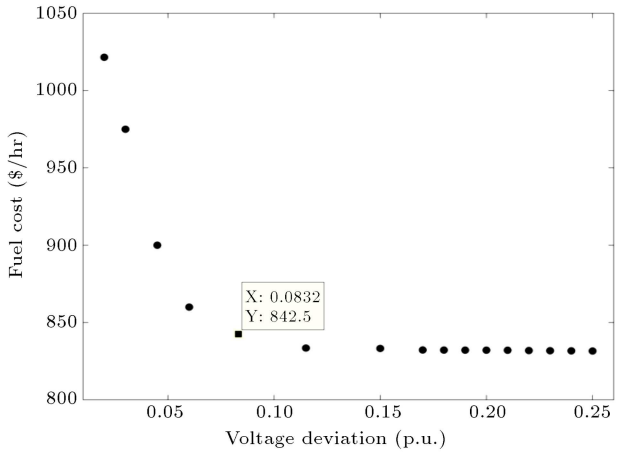

Figure 21. Pareto front for Test case 19.

used for the case described using Eq. (28). Results obtained for this test case are demonstrated in Table 14. The total FC achieved using QRSOS is 842.5288 $/hr, which is 2.05% higher than that in Test case 2.1, and VD is achieved as 0.0832 p.u., which is 85.41% less than that obtained for single-objective minimization of Test case 2.1. Figure 21 represents the Pareto-front for this case. No existing results are available in the literature for comparison.

Test case 20: OPF for minimizing FC along with VD considering VE and POZ

Generator cost coefficients and POZs in Table 1 of [28] are used for the case described using Eq. (28). Results are presented in Table 14. The total FC achieved using QRSOS is 832.7439 $/hr, which is 0.904% higher, and VD is achieved as 0.1461 p.u., which is 74.70% lower when compared to the single-objective minimization of Test case 4. Figure 22 represents the Pareto-front for this case. No existing results are available in the literature for carrying out a comparative study of this case, too.

Analyses of the aforementioned case studies prove the supremacy of the proposed technique over other

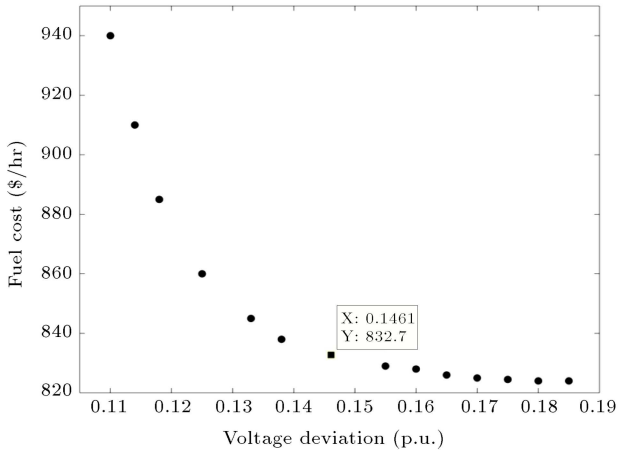

Figure 22. Pareto front for Test case 20.

algorithms such as QOTLBO, TLBO, MOHS, NSGA-II, ABC, BSA, PSO, DE-PSO, EP, IEP, GA, IABC, SA, SFLA, MSFLA, NLP, TS, ACO, Hybrid SFLA-SA, and SOS available in literature for achieving an optimum solution to the OPF problem. QRSOS produces superior solutions to other algorithms mentioned above for the cases studied. Pareto fronts obtained for each of the multi-objective functions depict solution sets well distributed in the search space, signifying a non-dominated solution.

6. Determining the best parameter settings for QRSOS

To determine the best parameter setting for QRSOS to deliver efficient results, population sizes of 10, 20, 30, 40, and 50 have been taken into consideration. For each population size, jumping rate JR is augmented from 0.1 to 0.9 in steps of 0.1, as shown in Table 18. Performance of QRSOS in Test case 4 is analyzed considering all the aforementioned combinations. Fifty different trials have been carried out with 100 iterations for each trial. Based on Table 18, it is observed that a population size of 30 and a Jumping Rate (JR) of 0.3 give the best fuel cost value of 825.2760 $/hr, which is less than previous best reported value of 825.3705 $/hr.

7. Statistical analysis of test results

Statistical analysis is done on 50 trial data sets to assess the performance of QRSOS. For this purpose, one trial data set, as obtained from the solution sets of the proposed algorithm, is tested using Wilcoxon Signed Rank Test (WSRT). A p-value (probability value) below 0.05 obtained from this test is considered as conclusive proof to counter the null hypothesis. p-values obtained using this test for Test cases 1-4 along with minimum, maximum, average values and standard deviation are tabulated below.

Table 18. Best parameter setting for QRSOS.

Population size	Jumping Rate (JR)									
	0.1	0.2	**0.3**	0.4	0.5	0.6	0.7	0.8	0.9	1
10	826.5956	826.5543	826.5142	826.5492	826.6166	826.6473	826.6759	826.6921	826.7051	826.7149
20	826.4182	826.3762	826.3651	826.4960	826.6253	826.6395	826.6627	826.6863	826.7127	826.7248
30	825.5214	825.4075	**825.2760**	825.3153	825.3752	825.4242	825.4621	825.4875	825.5023	825.6942
40	825.5193	825.4695	825.4473	825.4752	825.4763	825.4954	825.5121	825.5274	825.5331	825.5781
50	825.5403	825.5325	825.4620	825.4854	825.4891	825.4902	825.5123	825.5179	825.5194	825.5344

Table 19. Statistical analysis of QRSOS for single objectives using Wilcoxon signed rank test against 50 trials.

Test cases	Minimum	Average	Maximum	No. of hits to minimum solution	Standard deviation	p-value
Case 1	798.9152	798.9439	799.0110	35	0.0443	1.12E-10
Case 2.1	825.2541	825.2866	825.4346	41	0.0700	3.66E-11
Case 2.2	920.1125	920.1514	920.3242	40	0.0828	5.96E-11
Case 3	801.7593	801.7668	801.8001	40	0.0160	5.96E-11
Case 4	825.2769	825.2785	825.2865	38	0.0045	6.92E-11

As observed in Table 19, p-value in every case is well below the desired value of 0.05 establishing statistical significance of the results. Moreover, the standard deviation values obtained for QRSOS are much lower than those obtained by its predecessor [28] for all the cases.

Conclusion

This study aimed to introduce a novel technique designated as quasi-reflected symbiotic organisms search algorithm (QRSOS) to solve the OPF problem. The technique was successfully applied to the OPF problem to solve both single-objective and bi-objective functions. Twenty different test cases were solved with and without considering the VE and POZs. Outputs obtained using QRSOS were compared with those obtained by SOS, QOTLBO, TLBO, MOHS, NSGA-II, DE, and PSO; several other techniques are reported in the literature. Results obtained demonstrate the efficiency and robustness of the offered technique in handling OPF problem for both small- and large-scale test systems. Results showed a remarkable improvement for QRSOS when compared to other available techniques. It passed the Wilcoxon signed rank test with very low p-values and established its statistical significance. It was simultaneously observed that this algorithm acquired very fast convergence in all cases when matching other techniques. Henceforth, it may be deduced that QRSOS algorithm is promising, and there is a possibility for future research in this direction considering other aspects of power system.

Future scope

The proposed technique has effectively handled both linear and non-linear objectives. Since QRSOS was shown as able to solve the OPF problem successfully, it might be further applied to solve OPF, considering renewables and uncertainty due to load demands under different contingency scenarios.

Acknowledgement

The authors would like to acknowledge the lab facilities provided by the Electrical Engineering Department for carrying out the research work.

References

1. De Carvalho, E.P., dos Santos, A., and Ma, T.F. "Reduced gradient method combined with augmented Lagrangian and barrier for the optimal power flow problem", *Applied Mathematics and Computation*, **200**(2), pp. 529-536 (2008).
2. Momoh, J.A., Adapa, R., and El-Hawary, M.E. "A review of selected optimal power flow literature to 1993. I. Nonlinear and quadratic programming approaches", *IEEE Transactions on Power Systems*, **14**(1), pp. 96-104 (1999).
3. Santos, A.J. and Da Costa, G.R.M. "Optimal-power-flow solution by Newton's method applied to an augmented Lagrangian function", *IEE Proceedings-Generation, Transmission and Distribution*, **142**(1), pp. 33-36 (1995).

4. Yan, X. and Quintana, V.H. "Improving an interior-point-based OPF by dynamic adjustments of step sizes and tolerances", *IEEE Transactions on Power Systems*, **14**(2), pp. 709-717 (1999).
5. Huneault, M. and Galiana, F.D. "A survey of the optimal power flow literature", *IEEE Transactions on Power Systems*, **6**(2), pp. 762-770 (1991).
6. Zhang, S. and Irving, M.R. "Enhanced Newton-Raphson algorithm for normal, controlled and optimal power flow solutions using column exchange techniques", *IEE Proceedings-Generation, Transmission and Distribution*, **141**(6), pp. 647-657 (1994).
7. Habibollahzadeh, H., Luo, G.X., and Semlyen, A. "Hydrothermal optimal power flow based on a combined linear and nonlinear programming methodology", *IEEE Transactions on Power Systems*, **4**(2), pp. 530-537 (1989).
8. Burchett, R.C., Happ, H.H., and Vierath, D.R. "Quadratically convergent optimal power flow", *IEEE Transactions on Power Apparatus and Systems*, **11**, pp. 3267-3275 (1984).
9. Yuryevich, J. and Wong, K.P. "Evolutionary programming based optimal power flow algorithm", *IEEE Transactions on Power Systems*, **14**(4), pp. 1245-1250 (1999).
10. Lai, L.L., Ma, J.T., Yokoyama, R., and Zhao, M. "Improved genetic algorithms for optimal power flow under both normal and contingent operation states", *International Journal of Electrical Power & Energy Systems*, **19**(5), pp. 287-292 (1997).
11. Swain, A.K. and Morris, A.S. "A novel hybrid evolutionary programming method for function optimization", In *Evolutionary Computation, Proceedings of the 2000 Congress, on IEEE*, **1**, pp. 699-705 (2000).
12. Abido, M.A. "Optimal power flow using particle swarm optimization", *International Journal of Electrical Power & Energy Systems*, **24**(7), pp. 563-571 (2002).
13. El Ela, A.A., Abido, M.A., and Spea, S.R. "Optimal power flow using differential evolution algorithm", *Electric Power Systems Research*, **80**(7), pp. 878-885 (2010).
14. Abido, M.A. "Optimal power flow using tabu search algorithm", *Electric Power Components and Systems*, **30**(5), pp. 469-483 (2002).
15. Cai, J., Ma, X., Li, L., Yang, Y., Peng, H., and Wang, X. "Chaotic ant swarm optimization to economic dispatch", *Electric Power Systems Research*, **77**(10), pp. 1373-1380 (2007).
16. Roy, P.K., Ghoshal, S.P., and Thakur, S.S. "Biogeography based optimization for multi-constraint optimal power flow with emission and non-smooth cost function", *Expert Systems with Applications*, **37**(12), pp. 8221-8228 (2010).
17. Tripathy, M. and Mishra, S. "Bacteria foraging-based solution to optimize both real power loss and voltage stability limit", *IEEE Transactions on Power Systems*, **22**(1), pp. 240-248 (2007).
18. Khazali, A.H. and Kalantar, M. "Optimal reactive power dispatch based on harmony search algorithm", *International Journal of Electrical Power & Energy Systems*, **33**(3), pp. 684-692 (2011).
19. Roy, P.K., Mandal, B., and Bhattacharya, K. "Gravitational search algorithm based optimal reactive power dispatch for voltage stability enhancement", *Electric Power Components and Systems*, **40**(9), pp. 956-976 (2012).
20. Basu, M. "Teaching-learning-based optimization algorithm for multi-area economic dispatch", *Energy*, **68**, pp. 21-28 (2014).
21. Mandal, B. and Roy, P.K. "Multi-objective optimal power flow using quasi-oppositional teaching learning based optimization", *Applied Soft Computing*, **21**, pp. 590-606 (2014).
22. Abido, M.A. "Multiobjective particle swarm optimization for optimal power flow problem", In *Handbook of Swarm Intelligence*, pp. 241-268, Springer Berlin Heidelberg (2011).
23. Hernandez, Y.R. and Hiyama, T. "Minimization of voltage deviations, power losses and control actions in a transmission power system", In *Intelligent System Applications to Power Systems*, 2009. ISAP'09. *15th International Conference on*, pp. 1-5, IEEE (November 2009).
24. Roy, P.K., Ghoshal, S.P., and Thakur, S.S. "Multi-objective optimal power flow using biogeography-based optimization", *Electric Power Components and Systems*, **38**(12), pp. 1406-1426 (2010).
25. Sivasubramani, S. and Swarup, K.S. "Multi-objective harmony search algorithm for optimal power flow problem", *International Journal of Electrical Power & Energy Systems*, **33**(3), pp. 745-752 (2011).
26. Bhattacharya, A. and Chattopadhyay, P.K. "Application of biogeography-based optimisation to solve different optimal power flow problems", *IET Generation, Transmission & Distribution*, **5**(1), pp. 70-80 (2011).
27. Cheng, M.Y. and Prayogo, D. "Symbiotic organisms search: a new metaheuristic optimization algorithm", *Computers & Structures*, **139**, pp. 98-112 (2014).
28. Duman, S. "Symbiotic organisms search algorithm for optimal power flow problem based on valve-point effect and prohibited zones", *Neural Computing and Applications*, pp. 1-15 (2016).
29. Tizhoosh, H.R. "Opposition-based learning: a new scheme for machine intelligence", In *Computational Intelligence for Modelling, Control and Automation, 2005 and International Conference on Intelligent Agents, Web Technologies and Internet Commerce, International Conference on*, **1**, pp. 695-701, IEEE (November 2005).
30. Rahnamayan, S., Tizhoosh, H.R., and Salama, M.M. "Quasi-oppositional differential evolution", In *Evolutionary Computation, 2007. CEC 2007. IEEE Congress on*, pp. 2229-2236, IEEE (September 2007).

31. Ergezer, M., Simon, D., and Du, D. "Oppositional biogeography-based optimization", In *Systems, Man and Cybernetics, 2009. SMC 2009. IEEE International Conference on* pp. 1009-1014, IEEE (October 2009).
32. Zhang, C., Ni, Z., Wu, Z., and Gu, L. "A novel swarm model with quasi-oppositional particle", In *Information Technology and Applications, 2009. IFITA'09. International Forum on*, **1**, pp. 325-330, IEEE (May 2009).
33. Alsac, O. and Stott, B. "Optimal load flow with steady-state security", *IEEE Transactions on Power Apparatus and Systems*, **3**, pp. 745-751 (1974).
34. Kılıç, U. "Backtracking search algorithm-based optimal power flow with valve point effect and prohibited zones", *Electrical Engineering*, **97**(2), pp. 101-110 (2015).
35. Narimani, M.R., Azizipanah-Abarghooee, R., Zoghdar-Moghadam-Shahrekohne, B., and Gholami, K. "A novel approach to multi-objective optimal power flow by a new hybrid optimization algorithm considering generator constraints and multi-fuel type", *Energy*, **49**, pp. 119-136 (2013).
36. Bakirtzis, A.G., Biskas, P.N., Zoumas, C.E., and Petridis, V. "Optimal power flow by enhanced genetic algorithm", *IEEE Transactions on Power Systems*, **17**(2), pp. 229-236 (2002).
37. Saini, A., Chaturvedi, D.K., and Saxena, A.K. "Optimal power flow solution: a GA-fuzzy system approach", *International Journal of Emerging Electric Power Systems*, **5**(2), pp. 1-21 (2006).
38. Niknam, T., Rasoul Narimani, M., Jabbari, M., and Malekpour, A.R. "A modified shuffle frog leaping algorithm for multi-objective optimal power flow", *Energy,* **36**(11), pp. 6420-6432 (2011).
39. Ongsakul, W. and Bhasaputra, P. "Optimal power flow with FACTS devices by hybrid TS/SA approach", *International Journal of Electrical Power & Energy Systems*, **24**(10), pp. 851-857 (2002).
40. Sayah, S. and Zehar, K. "Modified differential evolution algorithm for optimal power flow with non-smooth cost functions", *Energy Conversion and Management*, **49**(11), pp. 3036-3042 (2008).
41. Ongsakul, W. and Tantimaporn, T. "Optimal power flow by improved evolutionary programming", *Electric Power Components and Systems*, **34**(1), pp. 79-95 (2006).
42. Sood, Y.R. "Evolutionary programming based optimal power flow and its validation for deregulated power system analysis", *International Journal of Electrical Power & Energy Systems,* **29**(1), pp. 65-75 (2007).
43. Bouktir, T., Slimani, L., and Mahdad, B. "Optimal power dispatch for large scale power system using stochastic search algorithms", *International Journal of Power & Energy Systems,* **28**(2), p. 118 (2008).
44. Yuryevich, J. and Wong, K.P. "Evolutionary programming based optimal power flow algorithm", *IEEE Transactions on Power Systems*, **14**(4), pp. 1245-1250 (1999).
45. Bouktir, T., Labdani, R., and Slimani, L. "Economic power dispatch of power system with pollution control using multiobjective particle swarm optimization", *Journal of Pure & Applied Sciences*, **4**(2), pp. 57-77 (2007).
46. Niknam, T., Narimani, M.R., Aghaei, J., Tabatabaei, S., and Nayeripour, M. "Modified honey bee mating optimisation to solve dynamic optimal power flow considering generator constraints", *IET Generation, Transmission & Distribution*, **5**(10), pp. 989-1002 (2011).
47. Abido, M.A. "Optimal power flow using tabu search algorithm", *Electric Power Components and Systems*, **30**(5), pp. 469-483 (2002).
48. Basu, M. "Multi-objective optimal power flow with FACTS devices", *Energy Conversion and Management,* **52**(2), pp. 903-910 (2011).
49. Malik, T.N., ul Asar, A., Wyne, M.F., and Akhtar, S. "A new hybrid approach for the solution of nonconvex economic dispatch problem with valve-point effects", *Electric Power Systems Research*, **80**(9), pp. 1128-1136 (2010).
50. Thitithamrongchai, C. and Eua-Arporn, B. "Self-adaptive differential evolution based optimal power flow for units with non-smooth fuel cost functions", *Journal of Electrical Systems*, **3**(2), pp. 88-99 (2007).
51. Özyön, S., Yaşar, C., Özcan, G., and Temurtaş, H. "An artificial bee colony algorithm (abc) approach to nonconvex economic power dispatch problems with valve point effect", In *National Conference on Electrical, Electronics and Computer (FEEB'11)*, pp. 294-299 (2011).
52. Yaşar, C. and Özyön, S. "A new hybrid approach for nonconvex economic dispatch problem with valve-point effect", *Energy,* **36**(10), pp. 5838-5845 (2011).
53. AydıN, D. and Özyön, S. "Solution to non-convex economic dispatch problem with valve point effects by incremental artificial bee colony with local search", *Applied Soft Computing*, **13**(5), pp. 2456-2466 (2013).
54. Wilcoxon, F. "Individual comparisons by ranking methods", *Biometrics Bulletin*, **1**(6), pp. 80-83 (1945).
55. Lee, F.N. and Breipohl, A.M. "Reserve constrained economic dispatch with prohibited operating zones", *IEEE Transactions on Power Systems*, **8**(1), pp. 246-254 (1993).
56. Niknam, Taher, Hasan Doagou Mojarrad, and Hamed Zeinoddini Meymand "Non-smooth economic dispatch computation by fuzzy and self adaptive particle swarm optimization", *Applied Soft Computing*, **11**(2), pp. 2805-2817 (2011).
57. Abaci, K. and Yamacli, V. "Differential search algorithm for solving multi-objective optimal power flow problem", *International Journal of Electrical Power & Energy Systems*, **79**, pp. 1-10 (2016).
58. *Data, IEEE 118-Bus Test System Data*, The Electrical and Computer Engineering Department, Illinois Institute of Technology, Available at: http://motor.ece.iit.edu/data/JEAS IEEE118.doc

59. Ghasemi, M., Ghavidel, S., Aghaei, J., Gitizadeh, M., and Falah, H. "Application of chaos-based chaotic invasive weed optimization techniques for environmental OPF problems in the power system", *Chaos, Solitons & Fractals*, **69**, pp. 271-284 (2014).

60. Ghasemi, M., Ghavidel, S., Rahmani, S., Roosta, A., and Falah, H. "A novel hybrid algorithm of imperialist competitive algorithm and teaching learning algorithm for optimal power flow problem with non-smooth cost functions", *Engineering Applications of Artificial Intelligence*, **29**, pp. 54-69 (2014).

61. Ghasemi, M., Ghavidel, S., Ghanbarian, M.M., Massrur, H.R., and Gharibzadeh, M. "Application of imperialist competitive algorithm with its modified techniques for multi-objective optimal power flow problem: a comparative study", *Information Sciences*, **281**, pp. 225-247 (2014).

62. Ghasemi, M., Ghavidel, S., Ghanbarian, M.M., Gharibzadeh, M., and Vahed, A.A. "Multi-objective optimal power flow considering the cost, emission, voltage deviation and power losses using multi-objective modified imperialist competitive algorithm", *Energy,* **78**, pp. 276-289 (2014).

63. Chaib, A.E., Bouchekara, H.R.E.H., Mehasni, R., and Abido, M.A. "Optimal power flow with emission and non-smooth cost functions using backtracking search optimization algorithm", *International Journal of Electrical Power & Energy Systems*, **81**, pp. 64-77 (2016).

64. Shaheen, A.M., El-Sehiemy, R.A., and Farrag, S.M. "Solving multi-objective optimal power flow problem via forced initialised differential evolution algorithm", *IET Generation, Transmission & Distribution,* **10**(7), pp. 1634-1647 (2016).

65. Reddy, S.S., Bijwe, P.R., and Abhyankar, A.R. "Faster evolutionary algorithm based optimal power flow using incremental variables", *International Journal of Electrical Power & Energy Systems*, **54**, pp. 198-210 (2014).

66. Reddy, S.S., Abhyankar, A.R., and Bijwe, P.R. "Reactive power price clearing using multi-objective optimization", *Energy*, **36**(5), pp. 3579-3589 (2011).

67. Reddy, S.S. and Rathnam, C.S. "Optimal power flow using glowworm swarm optimization", *International Journal of Electrical Power & Energy Systems,* **80**, pp. 128-139 (2016).

68. Reddy, S.S. and Bijwe, P.R. "Day-Ahead and Real Time Optimal Power Flow considering Renewable Energy Resources", *International Journal of Electrical Power & Energy Systems*, **82**, pp. 400-408 (2016).

69. Surender Reddy, S. "Optimal power flow with renewable energy resources including storage", *Electrical Engineering*, **99**(2), pp. 685-695 (2017).

70. Das, A.K., Majumdar, R., Panigrahi, B.K., and Reddy, S.S. "Optimal power flow for Indian 75 bus system using differential evolution", In *International Conference on Swarm, Evolutionary, and Memetic Computing*, pp. 110-118, Springer Berlin Heidelberg (December 2011).

71. Mandal, B. and Roy, P.K. "Optimal reactive power dispatch using quasi-oppositional teaching learning based optimization", *International Journal of Electrical Power & Energy Systems*, **53**, pp. 123-134 (2013).

72. Bhattacharya, A. and Chattopadhyay, P.K. "Solution of economic power dispatch problems using oppositional biogeography-based optimization", *Electric Power Components and Systems*, **38**(10), pp. 1139-1160 (2010).

Biographies

Anulekha Saha received her BTech degree in Electrical Engineering from Birbhum Institute of Engineering and Technology, India and MTech from the Department of Electrical Engineering, NIT Agartala in 2010 and 2012, respectively. Presently, she is a research scholar at the Department of Electrical Engineering, NIT Agartala. Her research area deals with power system optimization using various soft-computing techniques.

Ajoy Kumar Chakraborty received his LLE from the State Council of Engineering and Technical Education, West Bengal in 1979, B.E.E from Jadavpur University in 1987, MTech (Power System) from IIT Kharagpur in 1990, and PhD (Engg) in 2007 from Jadavpur University, respectively. He has sixteen years of teaching and fourteen years of industrial experiences. His areas of interest include application of soft computing techniques for different power system problems, Power Quality, FACTS & HVDC, and Deregulated Power System. He worked as a Professor with the college of Engineering & Management, Kolaghat; he is presently working as an Associate Professor at the Department of Electrical Engineering, NIT Agartala, India.

Priyanath Das obtained his BTech and MTech in Electrical Engineering in 1994 and 2002, respectively. He completed his PhD from Jadavpur University in 2013. He is presently working as an Associate Professor at the Department of Electrical Engineering, NIT Agartala, India. He has published several papers in national and international conferences and journals. His areas of interest include application of FACTS & HVDC, Deregulated Power System, and High Voltage Engineering.